Boreal Forest Wildfire in a Changing Climate

Eckdahl, Johan

2023

Boreal Forest Wildfire in a Changing Climate

JOHAN A. ECKDAHL
DEPARTMENT OF PHYSICAL GEOGRAPHY AND ECOSYSTEM SCIENCE | LUND UNIVERSITY

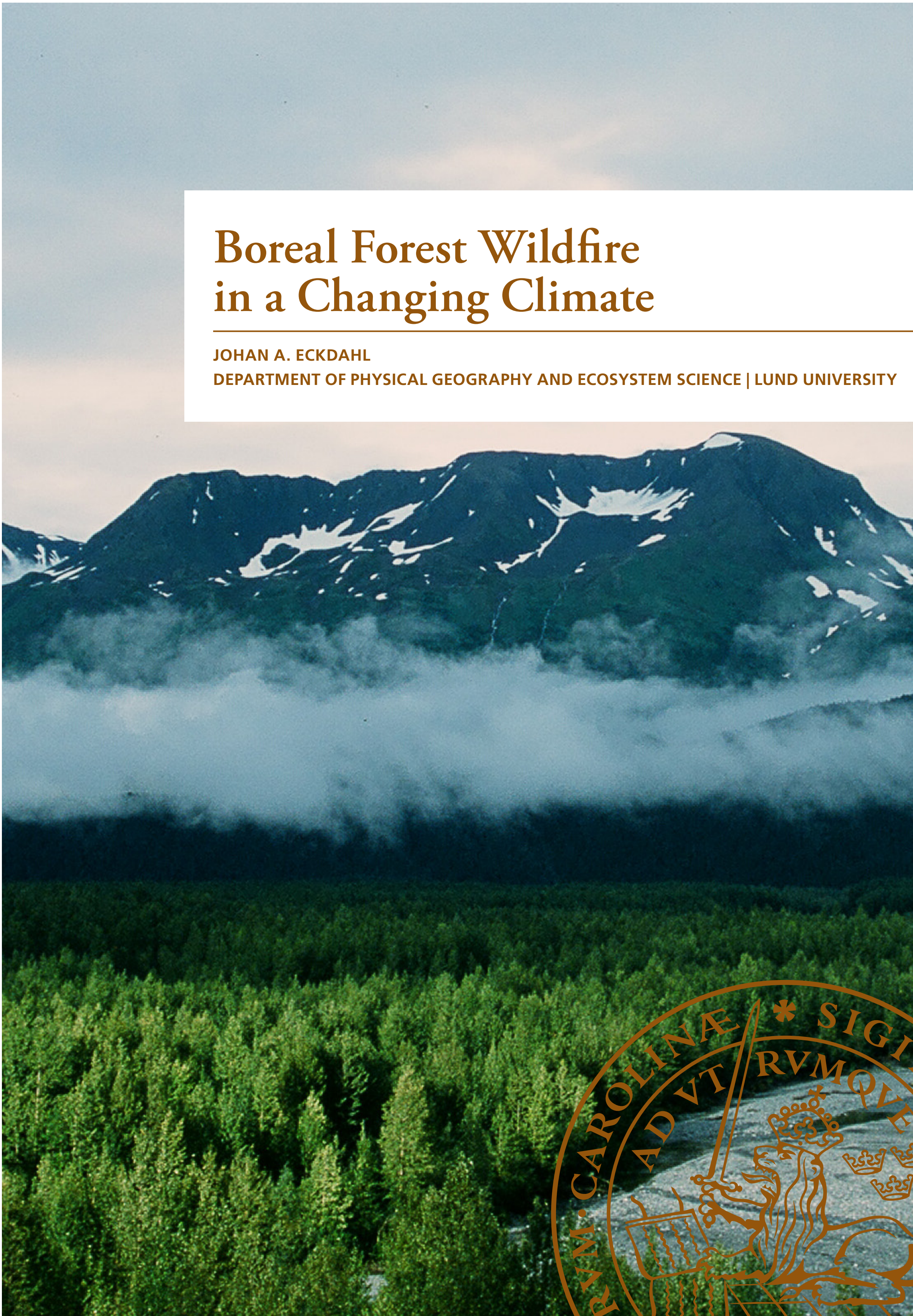

Boreal Forest Wildfire in a Changing Climate

Boreal Forest Wildfire in a Changing Climate

by Johan A. Eckdahl

Doctoral Dissertation
Thesis advisors: Prof. Daniel B. Metcalfe, Dr. Jeppe A. Kristensen
Department representative: Dr. Andreas Persson
Faculty opponent: Dr. Adam F. A. Pellegrini

Dissertation for the degree of Doctor of Philosophy (PhD) at the Faculty of Science of Lund University to be publicly defended on the 14th of February, 2024 at 10:00 in Pangea Hall at the Department of Physical Geography and Ecosystem Science.

Organization **LUND UNIVERSITY** Department of Physical Geography and Ecosystem Science Sölvegatan 12, Lund, Sweden	Document name **Doctoral Thesis**
	Date of disputation 2024-02-14
Author(s) Johan A. Eckdahl	Sponsoring organization

Title and subtitle
Boreal Forest Wildfire in a Changing Climate

Abstract
The boreal region contains 40% of the earth's carbon (C) that is stored in vegetation and soils with its forests accounting for almost 30% of the terrestrial C sink. Boreal forests are experiencing some of the most rapid rates of climatic warming and increases in fire activity, threatening to release large amounts of their dense C reserves to the atmosphere. While climate and wildfire place strong controls on ecosystem function, few observations have been made regarding their potential synergistic effects. This thesis utilized 50 separately occurring summer 2018 wildfires, each paired with an unburnt control and spread across the near-entire climatic range of boreal Fennoscandia, providing the first field campaign targeting regional-scale variation in boreal wildfire activity. It was found that climate determined the prefire quantity and structure of forest fuel, which in turn controlled both the immediate and extended fire-induced removal rates of C and nitrogen (N) to the surrounding land and atmosphere. Reorganization of ecosystem structure through wildfire burning strengthened climatic control over soil microbial community structure and nutrient cycling, with warmer regions experiencing enhanced nutrient mobilization under oligotrophic processing of remaining burnt organic soil. Greater warmth and soil fertility together stimulated growth of broadleaf overstory species under a restricted recovery capacity of previously established coniferous and ericaceous plant communities, though this transition to novel growth patterns was limited by residual, biodiversity inhibiting plant-soil feedbacks. Together these results suggest that continued climate change and wildfire can serve to remove C and nutrients from burnt boreal forests under a limited capacity for their reaccumulation. This postfire resource drain is capable of influencing longer-term patterns of ecosystem regrowth and the boreal forest contribution to the global land-atmosphere C balance that is deserving of further study.

Key words
boreal forest wildfire, carbon emissions, nutrient cycling, nitrogen, microbial community, plant community, climate change, secondary succession, Sweden, Fennoscandia

Classification system and/or index terms (if any)		
Supplementary bibliographical information		Language English
ISSN and key title		ISBN 978-91-89187-31-3 (print) 978-91-89187-32-0 (pdf)
Recipient's notes	Number of pages 179	Price
	Security classification	

Signature ______________________ Date 2023-11-15

Boreal Forest Wildfire in a Changing Climate

by Johan A. Eckdahl

LUND UNIVERSITY

A doctoral thesis at a university in Sweden takes either the form of a single, cohesive research study (monograph) or a summary of research papers (compilation thesis), which the doctoral student has written alone or together with one or several other authors.

In the latter case the thesis consists of two parts. An introductory text puts the research work into context and summarizes the main points of the papers. Then, the research publications themselves are reproduced, together with a description of the individual contributions of the authors. The research papers may either have been already published or are manuscripts at various stages (in press, submitted, or in draft).

Cover front: Photo of Exit Glacier in the Kenai Mountains taken by Johan Eckdahl on Portra 400 while visiting his father in Alaska.

Cover back: Photo taken by Jay Christensen near Denali in Alaska.

Funding information: Thesis work was financially supported by the interdisciplinary strategic research environment Biodiversity and Ecosystem Services in a Changing Climate (BECC).

Faculty of Science, Department of Physical Geography and Ecosystem Science

isbn: 978-91-89187-31-3 (print)
isbn: 978-91-89187-32-0 (pdf)

Printed in Sweden by Media-Tryck, Lund University, Lund 2023

Wanderer, there is no path ahead,
you make the path by walking.
–Antonio Machado

Contents

List of papers

This thesis is built upon the following papers, referred to by their Roman numerals. Papers I, II and III were published and reproduced under the Creative Commons Attribution 4.0 License (CC BY 4.0). Paper IV is an unpublished manuscript with reproduction rights reserved by the authors.

I **Climatic variation drives loss and restructuring of carbon and nitrogen in boreal forest wildfire**
J. A. Eckdahl, J. A. Kristensen, D. B. Metcalfe
(2022) *Biogeosciences*, 19, 2487-2506.

II **Mineral Soils Are an Important Intermediate Storage Pool of Black Carbon in Fennoscandian Boreal Forests**
J. A. Eckdahl, P. C. Rodriguez, J. A. Kristensen, D. B. Metcalfe, K. Ljung
(2022) *Global Biogeochemical Cycles*, 36, e2022GB007489.

III **Climate and forest properties explain wildfire impact on microbial community and nutrient mobilization in boreal soil**
J. A. Eckdahl, J. A. Kristensen, D. B. Metcalfe
(2023) *Front. For. Glob. Change* 6:1136354.

IV **Plant biodiversity limits carbon recapture after wildfire in warming boreal forests**
J. A. Eckdahl, J. A. Kristensen, D. B. Metcalfe

The following papers published during the doctoral program are not included in the thesis:

The DAQ system of the 12,000 channel CMS high granularity calorimeter prototype CMS HGCAL collaboration 2021 *JINST* **16** T04001

Construction and commissioning of CMS CE prototype silicon modules CMS HGCAL collaboration 2021 *JINST* **16** T04002

Response of a CMS HGCAL silicon-pad electromagnetic calorimeter prototype to 20–300 GeV positrons CMS HGCAL collaboration 2022 *JINST* 17 P05022

Author contributions

Author contributions are tabulated using CRediT (Contributor Roles Taxonomy).

Conceptualization – Ideas; formulation or evolution of overarching research goals and aims.
Data curation – Management activities to annotate (produce metadata), scrub data and maintain research data (including software code, where it is necessary for interpreting the data itself) for initial use and later re-use.
Formal analysis – Application of statistical, mathematical, computational, or other formal techniques to analyze or synthesize study data.
Funding acquisition – Acquisition of the financial support for the project leading to this publication.
Investigation – Conducting a research and investigation process, specifically performing the experiments, or data / evidence collection.
Methodology – Development or design of methodology; creation of models.
Project administration – Management and coordination responsibility for the research activity planning and execution.
Resources – Provision of study materials, reagents, materials, patients, laboratory samples, animals, instrumentation, computing resources, or other analysis tools.
Software – Programming, software development; designing computer programs; implementation of the computer code and supporting algorithms; testing of existing code components.
Supervision – Oversight and leadership responsibility for the research activity planning and execution, including mentorship external to the core team.
Validation – Verification, whether as a part of the activity or separate, of the overall replication / reproducibility of results / experiments and other research outputs.
Visualization – Preparation, creation and / or presentation of the published work, specifically visualization / data presentation.
Writing – original draft – Preparation, creation and / or presentation of the published work, specifically writing the initial draft (including substantive translation).
Writing – review & editing – Preparation, creation and / or presentation of the published work by those from the original research group, specifically critical review, commentary or revision – including pre- or post-publication stages.

	Paper I	Paper II	Paper III	Paper IV
conceptualization	JE, JK, DM	JE, JK, DM, KL	JE, JK, DM	JE
data curation	JE	JE, PCR	JE	JE
formal analysis	JE	JE	JE	JE
funding acquisition	JK, DM	JK, DM, KL	JK, DM	JK, DM
investigation	JE, JK, DM	PCR, KL	JE, JK, DM	JE
methodology	JE, JK, DM	JE, KL	JE, JK, DM	JE
project administration	JE, JK, DM	JE, KL	JE, JK, DM	JE, JK, DM
resources	JE, DM	JE, KL	JE	JE
software	JE	JE	JE	JE
supervision	JE, JK, DM	KL	JE, JK, DM	JE, JK, DM
validation	JE, JK, DM	KL	JE	JE
visualization	JE	JE, JK	JE	JE
original draft	JE	JE	JE	JE
review and editing	JE, JK, DM	JE, JK, DM, KL	JE, JK, DM	JE, JK, DM

Popular science summary in English

The boreal forests of the north have accumulated vast stores of carbon from the atmosphere over thousands of years due to higher rates of plant growth than decomposition. This sink of carbon has been important for stabilizing the global climate by maintaining the greenhouse gas content of the atmosphere. However, increased wildfire activity associated with recent climate change is threatening to release boreal carbon stores to the atmosphere at rates faster than they can reaccumulate, further driving climatic instability. Though much more research is needed in order to predict in greater detail the mechanisms by which climate change will alter the characteristics of boreal forests and their overall ability to sequester carbon.

A rare opportunity presented itself in 2018 when the near-entire range of boreal forests in Sweden experienced high fire activity. This allowed for burnt conifer forest properties to be measured in the field across 50 wildfire events which spanned wide ranges of mean annual temperature and precipitation. These measurements were compared to 50 unburnt forests that were matched to each burnt site to serve as an estimate of their prefire conditions. The resulting scientific analyses presented in this thesis provide one of the most comprehensive views into how changes in climate can influence the impact of wildfire on boreal forests.

It was found that in the years leading up to a fire event, climate can determine the distribution of carbon within plants and soil and its relative amount compared to the important nutrient nitrogen. This arrangement of material determined what was combusted during burning, with warmer regions tending to preserve more nitrogen than carbon. Faster break down of excess nitrogen-containing material by microbes under warmer conditions was important for fertilizing the soil, allowing more nutrient-demanding and quickly growing broadleaf trees to grow in place of the previously established needle-leaved conifers in the burnt forests. However, conifer forest soil left after wildfire was poorly suited for broadleaf sprouting, preventing them from fully utilizing the extra nutrients that were available, which limited forest transition towards more temperate vegetation. This means that warming associated with climate change can increase rates of decomposition relative to plant growth in boreal forests, shifting them towards emitting large amounts of greenhouse gasses to the atmosphere and further accelerating climate change. This thesis provides important advances in knowledge regarding the role of climate and wildfire in influencing the cycling of the chemical elements in boreal forests, thereby improving understanding of their contributions to the global carbon cycle.

Populärvetenskaplig sammanfattning på svenska

De boreala skogarna i Norden har samlat en stor mängd kol från atmosfären över tusentals år på grund av en oproportionerlig hög planttillväxt i förhållande till nedbrytning. Den här kolsänkan har varit viktigt för att stabilisera det globala klimatet genom att reglera atmosfärens växthusgasinnehåll. Ökad skogsbrandsaktivitet kopplad till aktuell klimatförändring hotar att släppa ut borealt kol till atmosfären snabbare än det kan återackumuleras, en process som driver klimatinstabilitet. Mycket mer forskring krävs för att förstå mekanismerna att klimatförändring kommer att justera de boreala skogarnas förmåga att lagra kol.

En viktig möjlighet dök upp år 2018 då nästan hela det boreala området i Sverige upplevde hög brandaktivitet. Den här situationen tillät barrskogar att mättas i fältet över 50 skogsbränder som fanns över ett brett spektrum av medeltemperatur och nederbörd. De här mätningarna jämfördes mot 50 obrända skogar, matchade mot varje bränd skog för att uppskatta deras förhållanden innan branden.

Det visade sig att under åren ledande till en skogsbrand kan klimat styra hur kol distribueras mellan växter och jord och dess relativa mängd jämfört med den viktiga näringen kväve. Den här fördelningen av material bestämde det som brann, med varmare regioner som tenderade att hålla kvar mer kväve än kol. Snabbare mikrobiell nedbrytning av material med hög kväve under högre temperatur var viktigt för att berika jorden. Det här gjorde att mer näringskrävande och snabbväxande lövträd kunde växa istället för de tidigare barrträden i de brända skogarna. Men jord anpassad till barrträd som lämnades kvar efter skogsbränderna var inte optimal för lövträd att gro i, vilket hindrade dem från att utnyttja extra näring och växa till sina fulla kapicitet. Det här innebär att varmare temperaturer, kopplade till klimatförändringar, kan öka nedbrytninghastigheten i förhållande till planttillväxt, och därmed öka växthusgas uttsläpp till atmosfären. Den här avhandlingen presenterar viktiga steg framåt för att förstå klimatets roll i att påverka biogeokemiska cykler i boreala skogar och deras koppling till den globala kolcykeln.

Acknowledgements

Long ago my family emerged from deep within the forests of Blekinge, crossing the vast ocean and rugged North American landscape to resettle in Los Angeles. There, when I was very young, my grandmother opened a bank account for me to save up for school. I put quarters in at time, all the while she would keep me on the phone for hours, quizzing me with brain teasers that she found in the checkout aisle at the grocery store. My grandpa would try to teach me linear algebra, at a time when I could yet hardly read. And my uncle would be sure to show up on the regular to demonstrate how to take everything in the house apart, only sometimes helping to put it back together, then sweep me off into mountains where I learned some of the most valuable lessons of all. I miss you all so dearly, and I see in everything around all that you've given me. You are the lens through which I make clear this world.

And to my parents who have been a never-ending source of support in providing what I need to grow, I can never thank you enough. Because there are giving people like you, I will always reach higher and work towards the things I believe in. And of it all, you gave me my brother, who is the best friend I could have ever asked for. James, it's been so much fun to grow up with you and I'm so proud to see the thoughtful and dedicated person you've become. I wish I had the words for all those back home who are important to me, but I especially want to thank Carol and Jim for continuing to share their lives with me even at such a distance. Thank you to Chris, Butch, Erik and Jessica for welcoming me in Oregon through the hurdles of the pandemic. Those times in the forests and by the rivers were so important for building perseverance, and make it all the more difficult to even begin to imagine who I would be without my family.

I have met so many great friends in Sweden, and finding only a few words at a time to lend them will always be a challenge. Though I want to thank Emily for being one of the most fun and adventurous people I've ever met, and for your ability to self reflect, always finding some way forward to grow and be a better person. Thank you Tamara for being so inspiring of generosity and teamwork, and for being such a solid source of good times through whatever life has thrown our way. I have learned a lot from you! Femke, you are one of the kindest people I've ever met, and have always been an important reminder to stay focused on the things that matter most. Thank you to Andrea and Tove for being a great example of love and care in my life, you make me believe that all good things are possible. Armand and Javier, you could be way worse, so thanks for not being that. Just kidding, you rule, and have been more important to me these many years than you might know. No, Bernice, the cat peeing on my backpack in Switzerland is not the first thing that comes to mind when thinking of you, it is your hard-working and tough attitude combined with a righteous love for altitude that does. Thanks for being such an inspiration. I've really enjoyed watching you grow as a person, Lovisa, and I admire the courage you show as you move ever closer towards levels of self-understanding that we all can look up to. Thanks Ágnes for all the "artistic" experiences, you remind me how good weird and weird good can be. Agge BNB, it has been an honor joining forces to make the everyday as suggestive as possible. I feel like I've gotten to know you best through how you shape the things around you with your care, especially Phoenix. And Mr. Nils, you are adventure in human form, keeping l'esprit d'humour and the freedom of the hills alive inside of me! Though we have not been in close contact during this program I want to thank Matthew, Suzy, Georgía, Dana, Carlos and Tommy for your role in being there for me in what has brought me to where I am today. Thanks also to Orlando, Alexandra, Geert, Joel, Tristan, Enass, Jalisha, Erica, Albin, Carlos, Adrian, Albertas, Oleg, Antje, Klas, Deepak, Abhishek, Yanzi, Hani, Hannah, Rieke, Ling, Rebecca, Luiz, Sílvia and Leon from Lund and Adrian, Saúl, Tobi, Matouš, Juan-Ignacio, Alisa, Isolde, and Rich from Umeå for being people I've enjoyed so much knowing.

Dan and Jeppe, I appreciate your brave research approach, and doing big things in a simple way has been a great learning experience. Thank you Andreas for your dedicated support and positive input throughout the program. Thanks Kalle for your enthusiasm and reliability, teaming up with you and Pere has been really fun and it was cool how much we could do so quickly! Thanks Cecilia for your consistent support and care for us PhD students in Lund. Thank you to Patrik Vestin for all the kind help and advice over the years. You are a really great person who I look up to. Thanks Åsa Wallin, and Marcin Jackowicz-Korzynski for valuable technical assistance with sample processing. Thank you Michael Gundale, Martin Berggren, James Hagan, Ryan Sponseller, Jonatan Klaminder, Saúl Rodríguez Martínez, Sylvain Monteux, Makoto Kobayashi, Johan Nord, Veiko Lehsten, Sebastian Diehl, Anders Ahlström, Natascha Kljun, Julia Kelly, Margarida Soares and Md. Rafikul Islam for helpful discussion in developing this project. I appreciate the above-and-beyond support from Cecilia Vallin and Joanna Jonsson while working in Umeå. Thanks for fieldwork assistance from Femke Pijcke, Rieke Lo Madsen, Geerte Fälthammar-de Jong, Lotte Wendt, Julia Iwan, Neija Elvekjær, Mathias Welp, Caroline Hall and Henni Ylänne. Support was provided by representatives from SLU Umeå, Unibest, Skogsstyrelsen, and Myndigheten för Samhällsskydd och Beredskap (MSB). I would also like to thank Peter Sondhauss, Uwe Mueller, Mirko Milas, Giuseppe Bianco, Johan Bäckman, Dean White, Susanne Kyre, Joe Incandela, Laura Bylund, Robert Keil, Jana Johnson and the many great teachers I've had for their role in passing on what was needed to perform this research.

Lastly, I want to thank all those involved in the care of our natural world. There are difficult decisions to be made each day. How do we live in harmony within such a wildness? Much has been done in taming this wildness to our good health while leaving so much left for awe. Your work has imparted a sense of beauty that has been central in inspiring the authoring of this thesis.

I have had the opportunity of working with the largest and most advanced technology to measure the smallest and simplest phenomena we can imagine to now piecing together some of the most expansive and complex Earth processes with a shovel and ruler. And much in between. Despite many upsets, I have had great fortune within the bite I have taken out of life and the perspectives it has allowed me. Though such fortune is not equally distributed to all, and now more than ever I have a keen sense of the great responsibility held within the voice that fortune can give. I do hope that I have used this voice well in providing understanding that can help us to better live with our world around.

Boreal Forest Wildfire in a Changing Climate

Chapter 1

Research Aims

The aims of this thesis are simply motivated. We know the climate is changing. We know changing climate is connected to alterations in wildfire activity. And we know that climate and wildfire control the structure and function of boreal forests. Yet we do not know enough to be prepared for the coming decades of environmental instability. Most of our knowledge is pieced together additively from disparate studies that are both spatially and methodologically isolated. No direct attempt has been made in the field to observe the synergistic effects of climatic variation and wildfire burning on boreal forest ecosystems.

Furthermore, little emphasis has been placed on investigating the representativeness of accumulated knowledge over the large possible variation of fire processes that can occur in boreal forests as a whole. Understanding of boreal wildfire contribution to the global land-atmosphere greenhouse gas balance is largely derived from a few high-intensity burn complexes in North America and comparison of the drivers of burn dynamics at the intercontinental scale has so far been only superficial. The mechanisms of ecological integration with the distinctly low-intensity fire regime of boreal Eurasia in particular harbors ample room for exploration and is an important research target to further develop knowledge of the contributions of forests to the global carbon cycle.

This thesis contains the results of the most spatially dispersed wildfire field campaign ever performed in boreal forests. Sampling was carried out with the intention to isolate the interactions of carbon and nitrogen with postfire recovery of plant and microbial communities across the near-entire climatic range of boreal Sweden. A network of 50 separately occurring summer 2018 wildfires and 50 individually matched unburnt controls was developed to address three broad gaps in knowledge:

1. Can macroclimatic conditions determine the immediate role of wildfire burning in the redistribution and loss of carbon and nitrogen within boreal forests?
2. How does climate and wildfire restructuring of boreal forests affect the biotic cycling of chemical elements over the years following fire?
3. By what mechanisms can postfire reassembly of plant and microbial communities integrate into biogeochemical feedbacks under shifting climate and fire regimes?

These questions were addressed in four separate papers appended to this thesis. The papers are preceded by a background section aimed at developing the fundamental principles that drive Earth's biogeochemical cycles in order to provide a framework of deductive navigation for use in interpreting the connection of the current work into the larger body of scientific knowledge. A methods section follows, covering the two field campaigns and following data analysis that generated the four papers. A descriptive overview of each paper is then provided as summarized under the constraint of demonstrating their interconnection in addressing the three main research questions listed above.

Chapter 2

Background

2.1 Synthesis of the Elements and their Formation of Earth

In the beginning, there was energy, or something. Then there was space, probably. After came light, maybe. Finally, mass was formed, it can be speculated. From there, the universe began to operate closer to what we can currently observe. And we observe it to be cooling, releasing the celestial bodies from the confines of their own gravitation, resulting in the synthesis of the elements and emission of radiative energy[1]. Stars form from the gravitational collapse of molecular clouds, primarily composed of hydrogen (74% current baryonic mass of the universe) and helium (25%), remnant of nucleosynthesis occurring during only the first few minutes of the universe[2]. An immense crushing force provides pressure and temperature high enough to overcome the coulomb barrier, that is, elevated particle energies allow them to break through electrostatic repulsion and travel close enough to each other to be bound by the short-range strong nuclear force[3]. Nuclear fusion of hydrogen into helium produces an energetic counter pressure that resists gravitational collapse and sustains the reaction. The energy that manages to escape at the surface as thermal radiation warms surroundings by cooling the star. In some stars, the increasing pressure provided by the accumulation of less reactive helium in the core can cause a secondary ignition that begins to fuse this element into heavier ones such as carbon, oxygen, nitrogen and iron[3]. In their eventual death, these stars serve to feed surrounding nebulae with heavy elements, in turn shaping their formative potential.

The universe is connected, and internal and external perturbation of interstellar material can provide for its aggregation and eventual accretion, that is, the self-amplifying collection of matter through enhancement of gravitational density. This process results in the formation of distinct objects that can further cluster material at various distances along a rotating disk, with the center forming a star (or stars) and celestial bodies such as planets later forming at varied proximity[4,5]. While the elemental composition of a star system will be determined by that collected during accretion, the distribution of thermal energy across the accretion disk can determine its allocation. In the case of the solar system, planets forming with cooler temperatures due to greater distance from the sun accumulated larger quantities of solidified volatiles, namely hydrogen and helium (e.g., Jupiter). Yet those closer, such as the warm Earth, concentrated heavier elements such as iron, which melted upon planetary condensing and sank to form a heavy metal core spinning within a liquid bath of iron and nickel together encased by a molten mantle of mineral material[6]. As the planet cooled volatile compounds that were captured in the mantle, such as water (H_2O), diatomic nitrogen (N_2), and carbon dioxide (CO_2), were released and able to form an atmosphere through the shielding of solar wind by the protective magnetic field of the rotating ferromagnetic core and gravitational attraction of the planet[7].

Eventually a surface crust solidified into tectonic plates subject to the convective activity of the mantle, forming drifting, rising and falling continents infilled by oceans[8]. This directed the inner earth to dissipate heat through gradual release of geothermal energy or explosive volcanic activity that further influenced atmospheric composition and added local variation to the mineralogy of the earth surface[9]. Together, outgassing, weathering, sedimentation and subduction of the earth's minerals formed geological cycles resembling those of today. The equilibration of these cycles has been a major factor in controlling the greenhouse gas content of the atmosphere, which in turn determines the receptivity of the atmosphere to Earth's dissipating heat[10]. Varied surface albedo and fluctuating insolation due to a spinning earth rotating on a tilted axis around the sun, forms latitudinally-dependent diurnal and seasonal cycles of energy input to the atmosphere, which is mixed convectively, forming chaotically fluctuating weather activity that can emerge as gradients of climatic patterns when integrated over space and time. This activity powers the redistribution of thermally responsive compounds, such as water, across the planet, granting gravitational potential energy to it, and that it carries, to shape the earth surface with erosive and corrosive power[11].

While many of the fine details leading to the formation of Earth are to always be shrouded in mystery, the principles will be the same. The universe has energy and mass with the space to distribute them. Time allows for their entropic rearrangement and the dissipation of gradients of energy. Energy can be extracted along these gradients to power stable cycles of mass transfer that drive diverse material self-organization that provides uncountable potential for emergent properties.

2.2 Emergence of Life

The earth is an extreme outlier among planets in how the intricate processes of its formation were able to provide for a rich arrangement of elements and continuously regenerating energy gradients that promote their cycling. Among these elements, carbon was particularly important in determining the land-atmosphere feedbacks that controlled the distribution of heat near the earth surface, as described above. Yet, for billions of years of tenancy this element hid its true potential in dictating the fate of the planet. Carbon has remarkably flexible bonding capabilities that allow for virtually infinite arrangements of stable molecular structure. Early in Earth history, the assembly of complicated carbon-based compounds was no more than a product of the random fluctuations of chemical synthesis and decay, though over long time local conglomerations of these compounds began to interact and eventually catalyze reactions among themselves[12]. These interactions were concentrated by their collection within self-constructed barriers (equivalent to the modern cell membrane), forming discrete units of activity that further accelerated the development of self-replicative abilities of organic structure[13]. Such organized, low-entropy conglomerations were far from thermodynamic equilibrium with their surroundings and a resulting drive towards spontaneous exchange of mass and energy with the environment demanded the development of mechanisms that maintain internal structure in the face of fluctuating external influence. The utilization of chemiosmotic gradients across lipid membranes appeared to be important in the development of the ability to convert external energy supply into usable chemical energy that contributed to the maintenance of thermodynamically dissipative structure, forming the basis for natural selection of adaptive metabolic processes that can maintain homeostasis of an organic entity under given environmental conditions[14]. Across the heterogeneous expanse of early Earth, this selection filter was broad, allowing a diversity of survival strategies to accumulate and coexist, spurring a multitude of interactions between them that further determined the propagation strategy and structure of organic material and its influence on the cycling of matter and energy. Together these processes formed the first semblances of units of life under ecological interaction and a precedent for the larger importance of carbon in the earth system.

One of the most significant advancements in the metabolic development of life was the advent of oxygenic photosynthesis[15]. This processes utilizes abundant solar radiation, water and CO_2 to produce chemical energy in the form of adenosine triphosphate (ATP) and reduced carbon together providing for cellular maintenance and growth. The rapid accumulation of energy and biomass made possible by this advent outcompeted anaerobic metabolisms, even poisoning them with the build up of highly reactive diatomic oxygen released during carbon fixation[16]. This process facilitated a sharp rise in atmospheric O_2 (along with reduced CO_2) inducing drops in global temperature and widespread extinction termed the "Great Oxygenation Event". This occurrence was one of the earliest examples of the extension of biotic processes into the larger earth cycles and the major impact that self-amplifying feedbacks can have on climate without stabilization mechanisms in place.

The oxygenation of the atmosphere selected for organisms that could harness its energy rather than be destroyed by it, directing the evolution of resistive biomass structure and highly efficient aerobic metabolisms capable of rapidly recycling photosynthetically derived material[16]. These advancements in efficiency were likely important for increasing the ability of individual organisms to coordinate and specialize their metabolic strategies to facilitate closed elemental cycles within communities. Tighter exchange networks may have been made further possible by the collection of facilitative metabolic activity into intermembrane space, as in initial abiogenesis. This trend of superorganismal activity and integration into more complex lifeforms continued to enhance flexibility to acquire and internally cycle resources, granting buffering capabilities of organisms to the perturbations of their environment[17]. These buffering capabilities in turn allowed organisms to expand their range into new territory or into competition within occupied ones[18]. Soon enough, a particular set of complex beings, capable of outcompeting all others with their technological advancements, came to power as orchestrators of the course of Earth's development. These creatures mined every corner of the earth for its resources, all the while indiscriminately polluting the land, water and atmosphere, contributing to climatic change and the reshaping of biotic communities through exaction of mass extinction. These beings were none other than plants.

2.3 Influence of Plants

The colonization of land by plants occurred over many millions of years and involved myriad evolutionary advances. These included the development of leaves that accelerated primary production as well as roots that shaped the formation of soils which could serve as a reservoir from which to insert and extract resources such as nutrient and moisture allowing for employment of strategic phenological pacing[19]. Soil development was likely immediately responsible for differentiation of plant strategy of resource exchange with this reservoir, especially in response to the diversity of parent material, microbial life and climatic conditions found across land. Of these strategies, the symbioses of plant roots with fungi, termed mycorrhizas, were likely of initial importance, as they are today[20]. These strategies are reminiscent of the early superorganismal biotic associations that merged to form the first complex life, though in this case the association was between already complex organisms, granting enormous potential for specialization and associative flexibility promoting their mutual success under broad ranges of environmental challenge[21]. Though not all plant-soil feedbacks were stable, and the imbalanced cycling of carbon between these two ecosystem compartments in particular has provided for dramatic impacts on the earth system throughout its history.

Specialization and improvement of enzyme efficiency allowed for the high biotic turnover of primary metabolites. For example, amino acids could be recycled through proteins in response to current gene expression and glucose could be quickly swapped between storage (e.g., starch) and structural forms (e.g., cellulose) during growth. The lability of these compounds granted flexible and rapid growth patterns to plants, though also made them susceptible to decay by external organisms and abiotic factors. This challenge drove development of secondary compounds that extended tissue longevity. Of these, lignin was particularly important for both the defense of plants from decay as well as the structural support that allowed them to reach taller and compete for access to light, forming the first trees and forest systems[22,23,24]. Synthesis of lignin incorporates structural irregularity and pre-oxidation that provides steric hindrance and limits development of specialized enzymes to reduce the activation energy required for its decomposition[22]. An outpacing of plant defense capabilities to rates of degradation from external influence may have been an important factor in allowing for the rapid expansion of vegetative biomass across the early land surface, producing a significant sink of carbon from the atmosphere with release of gaseous oxygen[24].

Eventually during this expansion, biomass accumulation was bound to become substantially inhibited by its own density under environmental constraint, though large sinks of atmospheric carbon could continue via the shedding and replacement of existing biomass of primary producers. However, much of this material would still be respired along a trophic chain stimulated by enhanced oxygen, forming a negative feedback for the sinking of carbon from the atmosphere. An added complexity to this feedback is the fact that primarily produced carbon has many opportunities to escape degradative conditions. Notably, its transfer to wet environments of limited gas exchange can enact rapid depletion of the high energy oxygen during respiration, forming strong gradients of chemical potential with a threshold at the atmospheric interface. Differential access to this energy of primary producers and decomposers can allow for accumulation of carbon and extension of its residence to the time-scales of sedimentation, presenting significant quantities for transfer from the fast (biosphere-atmosphere) to the slow (geological) carbon cycle further preventing their reaction with elevating O_2[25,26]. Indeed, periods of high moisture on land and large areas of shallow water bodies have provided for the movement of organic carbon to the geological cycle responsible for elevating atmospheric oxygen to up to 35% volume, compared to today's 21%[26,27]. These periods starkly demonstrated the importance of balances of biotic activity in the production and arrangement of varied carbon compounds across habitat configurations that serve to both pump carbon through the fast and to the slow carbon cycles and produce substantial impact on the energy content of the atmosphere (i.e., thermal vs. chemical). Furthermore, these processes represent one of the first clear signals of the formation of the modern patterns of connectance of small ecological scales (e.g., microbial) to those of larger space and time.

2.4 The Phenomenon of Wildfire

While the energizing of the atmosphere may have provided a strong driving force for the coming to dominance of plant life, it was not without its dangers. The bringing into proximity of molecular oxygen and reduced carbon forms an electrochemical gradient akin to the charging of a battery. Proper enzymatic circuity connecting its terminals can provide for the controlled and efficient transfer of energy into biologically usable forms (e.g., ATP)[28]. Though this circuit is liable to shorts, allowing oxidation of organic material to release unreined thermal energy into its surroundings. At suitable oxygen concentrations, such as at the interface with the atmosphere, this heat can provide activation energy for further oxidative decay of organic fuel, stimulating a chain reaction called fire. Fire is thought to have interacted with land plants since their conception, with atmospheric oxygen concentrations of at least 16% allowing for the propagation of wildfire across the landscape and a significant return of fixed carbon as gas to the atmosphere[29]. The intensity of combustion reactions are enhanced by oxygen concentration, allowing more widespread and destructive occurrence[29], forming a negative feedback for plant growth and associated carbon fixation and oxygen release. This feedback provided further evolutionary stimulus for the specialization of plants into five fire-adaptation strategies observed today[30]. Fire "embracers" do little to reduce their flammability and instead depend on senescence and competitive propagation to recover their population. "Endurers" suffer damage from fire, but retain the ability to quickly resprout from their surviving structure. "Colonizers" arrive on burn scars from off site using long-distance dispersal abilities. "Avoiders" adapt to areas that have reduced propensity to burning, namely through the storage of moisture that acts as a heat sink and stifles its delivery to the combustion reaction. Finally, "resisters" developed structure (e.g., thick bark, shedding dead branches) that suppressed burn intensity and reduced mortality through wildfire events, allowing their continued site residence and ability to recover their population through continuous recruitment. Though both at the species and community level these strategies were not mutually exclusive nor were they time-independent and thereby were able to organize alongside climatic conditions to enact reciprocal control on wildfire activity to produce regional fire regimes with characteristic return intervals and modes of burn propagation[31]. Many plant systems nestled into successive cycles of growth and destruction, with complex patterns of assembly and disintegration that could endure the challenges of largely unpredictable, though bounded, fluxes of energy input and extraction.

The added complexity of disturbances like burning to the dynamics of natural ecosystems is only beginning to be understood. Wildfire requires an ignition source to occur in the proximity of sufficiently arranged and desiccated fuel to allow for the adequate propagation of heat. For example, a lightning strike during dry weather can ignite a forest canopy, where a threshold of structural density will allow for accumulation of heat at rates faster than its dissipation. Energy that does escape regions of active combustion can serve to further dry and volatilize surrounding fuel, forming a highly combustible mixture of gas that accelerates the movement of the fire front to consume large land areas (often hectares to many km^2) of vegetation in high intensity flame. The ability of trees to control canopy structure, volatility and heat-dissipating moisture content in response to weather and climate will therefore be determinant of its burn dynamics, and even be able to direct burning away from the canopy to the forest floor[31]. Surface litter below the canopy will tend to be more closely configured, restricting gas exchange and resulting in less intense, but longer occurring burning due to its greater ability to store heat. Though this litter-derived fuel source will strongly reflect characteristics of the plants above, impacting volatility and combustion completeness under given burn conditions. Densely packed organic soil layers in the ground below will be more strongly influenced by the activity of microbiota and can even store enough heat to support smoldering combustion of weeks or more, compared to the minutes to hours typical of canopy fire[32,33,34,35,36]. Travel of fire through the forest vegetation, surface and ground present three very different modes of heat propagation and resulting impacts on the emission and transformation of ecosystem carbon.

Different fuel types and heating conditions will influence gaseous emission chemistry as well as the transformation of residual solid fuel[37]. For example, volatilized compounds can conglomerate into soot particles during combustion, providing physical obstruction to oxidation processes, forming highly refractory "black carbon"[38,39]. Solid fuels can conversely have specific surface area increased and be coated with partial negative charge, increasing its overall reactivity[38,39]. Though, the nearly unlimited transformation pathways of wildfire oxidation of organic material can direct it away from the specificity of degradative enzymes, reducing its decomposability. Yet, wildfire heat can also have a reverse effect of breaking down complicated molecular structure into that more easily integrated into microbial biomass[38,39]. Furthermore, differential thermolability of elements in fuel can cause their rebalancing, e.g., lower heating tends to preserve nitrogen relative to carbon, leaving behind highly nitrogenous pyrogenic material[40]. Nutrient enrichment can in turn nourish energy intensive biotic mineralization of refractory carbon post fire[41]. Lastly, the ability of wildfire to mobilize carbon to the atmosphere extends to the potential to alter its mobility through the land, eventually acting to amplify pumps from the fast to slow carbon cycles by transporting lowly reactive material to areas of sedimentation such as lakebeds and the ocean floor[42]. Therefore, initial fuel configuration enacts strong boundaries on the stochastic walk of wildfire heat propagation that provides for the material recomposition of an ecosystem that serves as foundation for the successional dynamic of biological communities and the cycling of carbon through the larger earth systems.

2.5 Forests in the Anthropocene

In the present day, forests cover 31% of the earth's land area[43]. These forests can be divided into three climatic regions: boreal, temperate and tropical. Growing season energy and length is largely determined by latitude and elevation and provides boundaries for life strategy and activity rates determinant of carbon allocation between biomass and soil pools. Within these regions carbon structure is further determined by gradients of moisture, a product of water inputs (e.g., inflow, precipitation) and outputs (e.g., evapotranspiration, drainage)[44]. While climate and topological factors do bound possibilities for ecosystem arrangement, and have been observed to explain distribution of carbon across the world's forests, the strategy and function of ecosystems as they develop under environmental limits can place further constraints on elemental cycling. Of these strategies, mycorrhizal associations appear to be important for determining the amount of carbon stored in soils, even offering greater statistical constraints on these quantities than climate at the global scale[45]. The two most studied mycorrhizas are the arbuscular mycorrhiza (AM) and ectomycorrhiza (EcM). AM and EcM can be considered as two strategies maintained by conglomerations of ecosystem feedbacks that form two ends of an axis of resource conservatism. Relative dominance of these strategies has been observed to shift smoothly across gradients of mean annual temperature[21]. The AM strategy relies on rapid turnover of organic matter and ability of AM fungi to infiltrate momentary openings in nutrient transfer between immobilized states over extended growing seasons for adequate delivery to their associated plants. The innate leakiness of high soil activity requires sustainable rates of resource replenishment found from, e.g., nutritious plant litter, root exudates, atmospheric nitrogen fixation and extraction from soil minerals[46]. In cooler regions with shorter growing seasons and more pressing demand to conserve available resources, a greater dominance of EcM arises, where EcM fungi monopolize root exudate supply and outcompete saprotrophs in the targeted mining of nutrient from the soil[47,48], enabling the indefinite accumulation of carbon on the forest floor in the absence of disturbance[49].

In boreal forests, relatively large amounts of soil carbon accumulation is a product of EcM dominance in response to the boundaries set by moisture and short growing seasons that limit soil activity. The accumulation of these dense ground stores lying across the vast expanse of the boreal region has long been a subject of interest as an important sink of carbon from the atmosphere[50]. Boreal forests are particularly fire prone and the ability to maintain their carbon sinking abilities is dependent on the frequency and severity of burning relative to rates of carbon accumulation. Because wildfire frequency and severity can vary, some forests sequester carbon over relatively long periods without burning while others can have nearly all their flammable carbon removed during highly destructive events earlier in their development. This varied burn severity and timing will produce differing recovery patterns. For example, complete to near-complete organic layer and conifer removal and elevated postfire nutrient cycling can promote stand replacement with broadleaves[51]. Over several decades, these broadleaves can gradually cede dominance to conifers under diminishing nutrient cycling rates in a process of relay succession[52]. This variability within a fire regime is responsible for producing landscapes with a mosaic of seral stages and burn severity, controlling forest recovery trajectories that stabilize under probabilistic distributions determined by regional climatic conditions and their associated patterns of fire weather. This stabilization provides for the adequate provisioning of genes to fill varying niche qualities and overall dimensionality over the course of recovery from destructive disturbance events[53]. Though boreal forests extend over large ranges of climate, bringing forth a comparatively extensive range of forest structure and associated fire response. In particular, lengthened growing seasons can allow for increased soil turnover and greater dominance of the AM strategy. AM associated plants tend to produce litter with lower carbon to nitrogen (C:N) ratios, which in turn may have altered flammability that controls the fire regime[45]. Furthermore, AM plants tend to form plant-soil feedbacks that encourage heterospecific plant germination, over EcM which restrict growth to conspecifics, and are thought to be important in determining latitudinal species diversity gradients[54]. Together, these mean that any alteration in local climate conditions can have cascading effects on the structure of boreal forests and a reshaping of their fire regimes, which can provide for disequilibrium between any of the small to large scale feedbacks that stabilize ecosystems across the landscape.

The mechanisms by which boreal forests can equilibrate to climatic flux is poorly understood, and complicated specifically by the influence of one particular lifeform intricately designed to be highly effective in undoing the severe alterations that plants had enacted on the land and atmosphere. This creature has fervently destroyed forests[43], and dug their long-buried waste from the earth, releasing it back into the atmosphere[55], effectively reversing pumps from the fast to slow carbon cycles. In just a couple hundred years this species alone was successful in increasing the carbon concentration of the atmosphere, disrupting climate systems that enacted more frequent and severe drought that further aided in the destruction of plant life[56]. During this period of change, high latitude regions have experienced particularly rapid rates of warming and increased fire activity that threaten to release long stored carbon in boreal forest vegetation and soils, creating a positive feedback with warming[57]. The creature became obsessed with monitoring their progress in the returning of the earth to its undisturbed, pre-plant state, enacting quests to indulge in the counting of every single atom of carbon released back into the atmosphere. These beings are none other than humans.

2.6 Monitoring Disequilibrium

Climate forcing due to the combustion of fossil fuels has caused severe disruption to ecosystems globally[56]. In particular, boreal forests across North America are experiencing increasing frequency of high-intensity wildfire that has the power to convert more land area from carbon sinks to sources[57]. Enhanced mean annual temperature and associated nutrient cycling, along with dwindling competitive abilities of conifers under mounting stress of induced maladaptation appears to be driving a transition towards greater deciduous dominance across the continent, with uncertain impacts on the future of ecosystem services such as carbon storage across the region[58]. More uncertainty arises at larger scale from the fact that fewer observations exist regarding the impact of shifting climate and fire regimes in boreal forests on the Eurasian continent despite containing 70% of the boreal land area[59]. Eurasian boreal forests historically have experienced lower intensity wildfire due to a greater prevalence of fire resisting overstory species, often restricting propagation to surface and ground fire[31]. While estimates of changes in total ecosystem N due to wildfire burning are rare in all boreal forests, pyrogenic material has been found to have enhanced C:N relative to its source material in North America compared to reduced C:N in Eurasia[60,61]. Relatively elevated nitrogen under less severe wildfire has the potential to increase microbial mobilization of this element that can fertilize postfire soils and potentially alter early postfire recovery patterns of plant species[41], a complicated phenomenon currently not well investigated compared to the more direct vegetation replacement via its total incineration in high-intensity wildfire.

High-intensity burning tends to extend over large areas of land once initiated and its frequency is expected to increase, justifying targeted research of this wildfire dynamic[62]. Though applying accumulated knowledge from this effort indiscriminately across the landscape has the potential to bias future understanding of flammable ecosystems globally. This is especially true when considering that fire frequency is bound to also increase at low intensities, potentially partly due to its entrance into systems traditionally protected from burning, like boreal wetlands, which can store vast amounts of carbon in the ground vulnerable to combustion when dried[63]. It is therefore crucial to understand the drivers and consequences of burn severity across its full range in order to predict and potentially reduce wildfire impact through careful landscape management as anthropogenic activity adjusts to shifting ecosystem services and regulates its influence on the environment. Furthermore, it must be acknowledged that traditional approaches to wildfire study tend to incorporate sampling within only single or closely grouped burn scars, resulting in a high potential for correlative trends to be entangled within the influence of pseudoreplication or spatial autocorrelation of uncertain or even uninvestigated extent[64]. These approaches also miss the influence of factors that vary coarsely over space, limiting insight into the connection of individual forest stands into their larger landscape and planet-wide feedbacks. In particular, despite the fact that both climate and wildfire regimes are separately known to strongly influence forest ecosystems, research has essentially been unseeing to their synergistic effects on forest structure and function, limiting predictive approaches regarding shifting forest dynamics under current trajectories of climatic change to only additive (rather than interactive) effects.

The performance of predictive models is ultimately determined by their degree of external validation, and both their accuracy and explanatory breadth can be increased by iterative adjustment to fit observations collected from the real-life systems they represent. The slow decadal change in climate paired with the suddenness and continuous novelty found within many of its consequences (e.g., wildfire, storm, drought, and pest events), make direct validation of predictive strategies crucial for human preparedness though often impossible, leaving models based on current Earth patterns with an unknown number of unknown unknowns. In such a position of information paucity, and a dire need for knowing, continuous and widespread exploratory environmental monitoring breaking traditional restrictions on spatial scale and level of abstraction is important for investigating ecosystems as they traverse an ever increasing global disequilibrium. Specifically, an eagerness to isolate ecological mechanism before establishing the emerging patterns they might construct[65], outdated and arbitrary distinction of ecosystem components, readiness to attribute unexplained variation to an insurmountable and innate stochasticity of nature, and ethos-based selection of research topic and methodology may currently hinder the ability to uncover important patterns emerging from the interactions of both known and unknown natural processes that improve the prediction and management of ecosystem services in the coming future.

The work presented in this thesis was designed to provide novel insight into the synergistic effects of climate and wildfire on biogeochemical cycling in boreal forests with implications for ecological trajectories of recovery under the coming decades of global change. This was completed using simple and repeatable monitoring methodology that sampled multiple interacting ecosystem components and processes across 50 mature forests spanning the near entire climatic range of boreal forest in Sweden, each paired with a nearby stand burnt during the nationwide wildfire outbreaks of summer 2018[66]. Minimal selection filters were placed on fire severity, allowing for capturing of a breadth of its variation across the region. The effects of this variation were sampled during the chaotic period of rapid ecosystem destruction and reconnection during the first two years after fire in attempts to understand how the immediate impacts of burning interact with the differential pace of recovery of ecosystem components as biota recolonize from both on and offsite refugia, across broad climatic control. The large sample sizes and diversity of variables provided for a flood of correlative patterns. To avoid model overfitting, data fishing and cumbersome management of caveats under an exploratory paradigm, a multitude of statistical approaches and theoretical abstractions were used to isolate only the most robust patterns of ecosystem connectivity as constrained by their ability to quantitatively explain the cycling of carbon and nitrogen. This perspective was seen less as a limitation in scope than a fundamental reference point by which to extend understanding of the important patterns of boreal forest intraconnection to the larger biogeochemical systems in which they are embedded, aiding in the effort to better predict their future in yet another period of great flux in the history of Earth.

Chapter 3

Methods

In 2018, abnormal weather pushed the near-entirety of Sweden into extreme drought. This allowed for large wildfires to break out across the near-entire forested region of the country. Contrasted to the fire season of 2014, where only a small portion of the country had dried enough for considerable fire activity, 2018 presented a rare opportunity to study the impacts of wildfire in a similar forest type (i.e., non-wetland, non-sloping, pine dominant, podzols), across broad gradients of climate.

The entirety of this thesis is built upon data derived from a network of 50 separate wildfires occurring during summer 2018 and paired unburnt controls spread across approximately 57-67° latitude, 0.43-7.77 °C mean annual temperature, and 539-772 mm mean annual precipitation (Figure 3.1). Sites were visited in approximate order of North to South during two field campaigns, the first spanning 5 to 20 August 2019, and the second over 29 July to 11 August 2020.

3.1 Plot Selection

The 50 burnt plots were selected to maximize spread across climate gradients within Sweden from a pool of 325 fires identified from the summer 2018 period that had perimeters manually mapped by the Swedish Forest Agency. Perimeters were drawn around burn scars delineated using Normalized Burn Ratio (NBR) values derived from Sentinel-2 bottom-of-atmosphere corrected bands 8 and 12. Close to the highest NBR pixel values in each separate burn scar, away from the immediate fire edges, one 20×20 m^2 plot was established along with an equally sized, paired control plot located in unburnt forest between 15 and 150 m (average 58 m) outside the burn scar. The control plots served as estimates of prefire properties for each of their corresponding

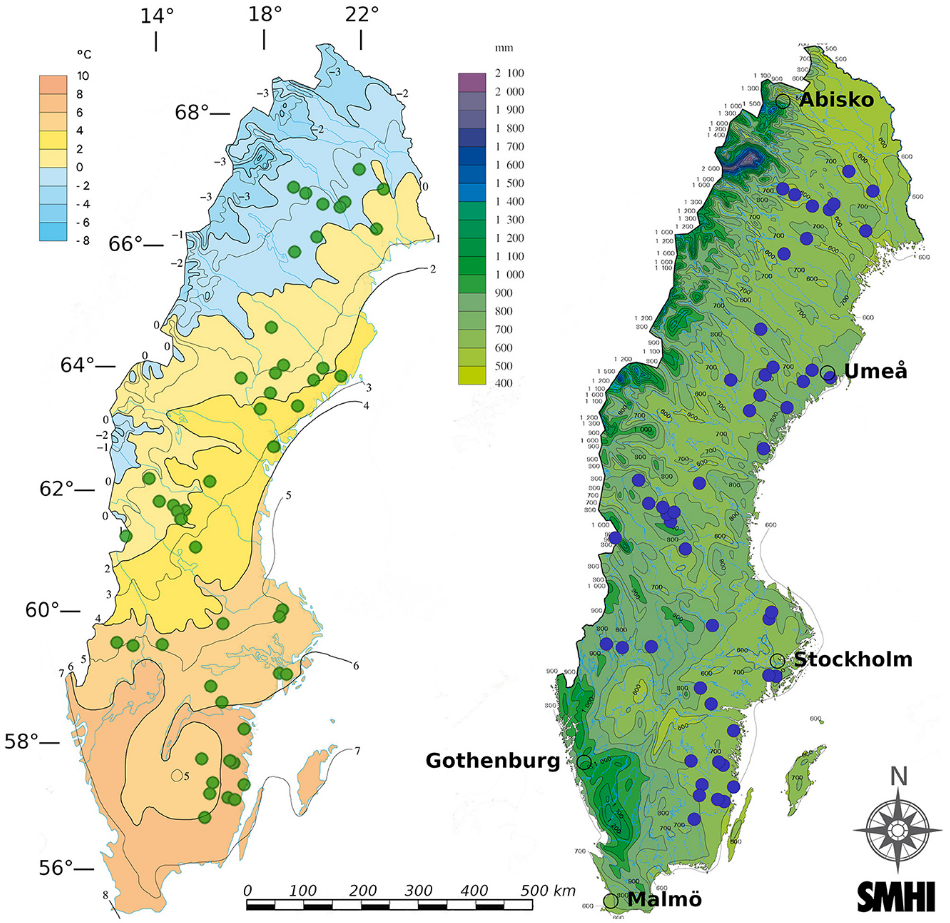

Figure 3.1: The 50 plot pairs spanned the approximately 57-67° latitudinal range within Sweden. They are seen as colored points on figures provided by the Swedish Meteorological and Hydrological Institute (SMHI) of mean annual temperature (left) and mean annual precipitation (right) over the last normal period 1961–1990. Major cities/research centers are marked with empty circle perimeters and WGS 84 (EPSG:4979) latitudes (horizontal bars) and longitudes (vertical bars) are given in degrees.

burnt plots. Visual satellite imagery was used to ensure there were no obvious changes in stand structure occurring between control and burnt plots. Using geodatasets prior to the field campaign, plot pairs were best matched to resemble each other in terms of overstory biomass, basal area, tree species dominance, and stand age, with these properties otherwise allowed to vary across the climatic and geographical span of the region. Topo-edaphically evaluated soil moisture potential (TEM), which was considered a metric of soil drainage, was also used to match plots and avoid wetland areas[67]. TEM was provided at 10 m resolution and given as integer values ranging from 0 to 240 (in order of increasing moisture potential) and was based on the Soil Topographic Wetness Index[68] in areas where soil type information was available and on the two topographic indices Depth to Water[69] and the Topographic Wetness Index[70] where soil information was unavailable. Elevation data was provided by the Swedish Mapping, Cadastral and Land Registration Authority from a 50 m resolution digital elevation model[71]. Slope was calculated using the "slope" function within the ArcGIS software environment[72]. All stands were located on minimally sloping land (less than 15° slope), and elevation change between plot pairs was minimized. The plot pairs were spread across broad gradients of mean annual temperature (MAT) and precipitation (MAP), ranging from 0.43-7.77 °C and 539-772 mm, respectively, during the years 1961-2017 (Figure 3.1).

3.2 Vegetation Sampling and Measurement

3.2.1 Overstory

In 2019 individual tree bole diameter (sampled at 130 cm height above the forest floor) and species were recorded within each plot perimeter for all trees of at least 5 cm diameter at measurement height. Trees less than 5 cm were uncommon and assumed to contribute negligibly to biomass and carbon (C) and nitrogen (N) emissions. A tree was recorded as living if standing upright and having any proportion of green needles[73]. If a fallen tree was charred only on its lower (in standing orientation) portions, it was deemed standing during fire ignition and its measurements were included if its base was within plot boundaries. In burnt plots, the percentage of brown and black needles in each tree canopy was visually approximated as 0%, 25%, 50%, 75%, or 100% with these individual values averaged to give an estimate of total plot canopy browning and blackening. Overstory biomass was calculated by entering bole diameters into allometric equations for Scots pine (*Pinus sylvestris*), Norway spruce (*Picea abies*), silver birch (*Betula pendula*), and downy birch (*Betula pubescens*)[74]. From the results of the equations, aboveground biomass was considered to be the categories stem wood, stem bark, living branches, dead branches, stump and needles while belowground was coarse roots ($\geq$ 5 cm) and fine roots ($<$ 5 cm). Stump, needle, coarse root and fine root categories were inapplicable for birch and its biomass was calculated only from the remaining categories. To estimate overstory total aboveground C and N, C_R (ratio of sample C weight to total weight) for all components was set to 0.5 and N_R (ratio of sample N weight to total weight) to 0.01 for needles and 0.004 for all other parts[75].

Plot-wide tree mortality (TMort) was calculated as the percentage of measured stems with no amount of green leaves in their respective canopies[73]. Species were also recorded, finding the 50 burnt plots to be largely dominated by Scots pine (*Pinus sylvestris*) with the percentage of Norway spruce (*Picea abies*) stems between 25%–50%

in five plots, between 50%–75% in three plots, and greater than 75% in two plots. Birch stems (*Betula pendula* and *Betula pubescens*) were less than 25% in 44 plots and between 25%–50% in six plots, of which only one was spruce dominant. All plots showed some visible charring of tree boles, though only three plots had greater than 1% plot-wide canopy blackening (i.e., evidence of time-of-fire canopy burning). The observed lack of charring in the canopy led to the assumption that the majority of the direct heating impact of fire was restricted to only the lower tree boles and flaming and smoldering combustion in the soil layers.

3.2.2 Understory

Understory samples were taken from control plots by cutting all non-moss, non-tree plant material at the surface of the soil within four 40×40 cm^2 patches, each from a separate plot quadrant. To reduce sampling error due to low plot coverage, the sample patches were chosen by performing four quadrant-wide surveys noting visual estimates of coverage and proportions of plant functional groups (i.e., graminoids, forbs, shrubs, and pteridophytes). These were applied in selecting representative patches for the portion of the quadrant that was vegetated, which was always all non-bare rock surface. The conglomerated biomass density and composition for the four samples were applied to the visually estimated non-bare rock surface area of an entire burnt plot to approximate its prefire understory coverage.

Aboveground understory vegetation was completely consumed in most burnt plots (causing a lack of variation for use in correlative analysis) and its prefire properties were therefore estimated by the paired control plots. There, understory was typically below 1 m in height and composed less than 2% of the C found in the soil when averaged across the 50 control plots.

3.2.3 Floristics

A floristics survey was performed for each of the 49 plots in summer 2020 (two years post fire) to capture the vegetation establishment stage[76]. Each plot was divided into quarters and a 40×40 cm sampling quadrat was placed randomly once in each of the four areas. All vegetation within the quadrat was clipped at the soil surface and stored. This procedure was performed again but with the plot split in two instead of four areas, resulting in a plot-wide conglomerated sample of six cuttings. One plot was sampled seven times, though all biomass values were divided by total sample area per plot to give units of g m^{-2}.

Each plot sample was dried for 3 days at 40 °C and dry weight recorded for use in analysis. For each of the 49 plots, the recorded species weights were divided into eight functional group categories including broadleaf (tree species only), conifer, pteridophyte, forb, and graminoid. Shrubs were split into three additional categories: ericaceous species that tend to resprout rhizomatously after fire (RhizErC, including *Vaccinium vitis-idaea, Vaccinium myrtillus*, and *Vaccinium uliginosum*)[77,78], ericaceous species that tend to germinate from seed (SeedErC)[79], and arbuscular mycorrhizal shrubs (ShrubAM). No moss or lichen biomass was found, with the forest floor below the regrowing plants being covered by a layer of char and some postfire additions of plant litter.

3.3 Soil Sampling and Measurement

During the first field campaign, sampling and analysis were broken into six forest compartments. The compartments included four soil layers (i.e., mineral, duff, moss/litter and char) as well as the two aboveground compartments (i.e., understory and overstory vegetation). The organic layer was defined as the duff, moss/litter and char layers grouped together while the soil category was considered as the organic layer grouped with the mineral layer. The category called "total" refers to the grouping of the soil and understory, but excludes the overstory due to its minimal combustion (as judged by observed scarcity of canopy blackening). Woody debris mixed in the moss/litter layer was sampled in this study, though not the coarse woody debris laying on top of this layer. While larger dead wood lying on top of the forest floor can contribute to C and N stocks and their losses due to fire, this material is typically of low prevalence in Sweden[80], difficult to accurately measure and standard methodology to estimate its consumption by fire is only beginning to be developed[81]. Therefore, focus was retained on the variation of the larger and more readily measurable ecosystem C and N pools in soil and living vegetation.

Soil horizon depths (i.e., the distance from bottom to top of each individual layer) of the mineral, duff, moss/litter, and char layers were measured at 20 points per plot from 10 equally spaced excavations along each plot diagonal[82]. The mineral layer was measured from its highest rock obtrusion to the bottom of the duff layer. The duff layer was considered the grouping of the F (partially decomposed material) and H (humic material) layers in accordance with the Canadian system of soil classification[83], as is common in boreal wildfire literature. The moss/litter layer was all unburnt material on top of the duff layer, including visually identifiable detritus and living moss. In all burnt sites, a layer of conglomerated char formed a clear boundary on top of the moss/litter allowing for distinct measurement. Here, char is defined as fully blackened, brittle material with apparent high heat exposure due to fire. This separation was made based on large observed differences in C and N concentrations in surface pyrogenic layers compared to lower residual layers in similar ecosystems[60,61,84]. All soils were podzols, except 6 which had no mineral soil across the measured transects and had organic layers directly on top of bedrock.

Samples were acquired for all four soil layers. Four mineral soil samples were taken using a 3 cm diameter, 40 cm long gouge auger corer at four corners of a square each 15 m from the plot center. Where feasible, at least 10 cm vertical mineral cores were taken, however in shallower layers a minimum depth of 5 cm each was collected. Duff samples were collected at the same plot corners as the mineral cores by excavating four soil volumes of approximately 25×25 cm^2 area and at least the full depth of the organic layer. This volume was trimmed to discard the mineral and moss/litter layers off the bottom and top of the volumes, respectively. Right angles were then gently cut with sharp scissors and the 3 dimensions were measured in millimeters (collected samples were at least 400 cm^3 each and aimed to sample the entire in situ depth). Duff and mineral soils were kept frozen until portions were freeze dried for separate analysis. Moss/litter samples were collected by cutting squares, with attention to preservation of the natural in situ volume, until filling a 553 cm^3 steel container. Char layer samples were similarly collected in a 112 cm^3 container. At least one sample each of moss/litter and char were acquired from each plot quadrant, though more were taken at equal spacing along a transect to fill the containers if the layer was thin. On the upper surface of the char layer were small portions of dry, unburnt material, which were likely postfire additions of litter to the forest floor. This material was discarded from the char collection and was not included in C and N stock estimates.

3.4 Site Temperature and Moisture Assessment

Under a given set of macroclimatic conditions, ecosystem structure can alter temperature in the subcanopy and soil which together may have a more direct effect than regional MAT on this study's sampled microbial, nutrient and forest properties. Three recently produced maps of mean annual temperature in the subcanopy at 15 cm above the forest floor[85] and in the soil between 0-5 cm depth and 5-15 cm[86] had strong multicollinearity with MAT in both control and burnt plots that was considered too great for these variables to be used together in statistical analysis ($r > 0.94$ for all). Soil and subcanopy temperatures were not found to be significantly different between burnt and control plots pairs due to soil maps having too low resolution (1 km) and subcanopy maps (25 m resolution) not incorporating the effects of the 2018 wildfires. Organic layer temperature and moisture (using a Delta-T HH2 meter and Thetaprobe type ML2x probe) were recorded at each plot center and four of its corners during the 2019 and 2020 field campaigns (plot pairs measured within at most 2 hours, northernmost plot-pair unmeasured due to salvage logging). No significant difference in moisture was found between burnt and control pairs in either year, though burnt plot soil temperature was significantly elevated in 2019 (1.34±0.28 °C) and 2020 (1.95±0.33 °C) at 95% confidence (two-tailed Z-test). These one-off measurements of moisture and temperature were not included in statistical analysis due to the highly variable nature of these soil properties over the year. Temperature logging ibuttons installed at 2 cm above the bottom of the organic layer found a temperature increase (averaged over time between the two site visits) of 0.39±0.16 °C in burnt plots relative to control in 23 plot pairs (two-tailed t-test at 95% confidence), though otherwise had too high a failure rate to provide adequate sample size for incorporation into analysis. Soil temperature and moisture conditions were therefore left to be approximated by variability in their larger-scale drivers including TEM (soil drainage), MAP (precipitation input), MAT (evapotranspiration) and TMort (albedo, soil solar insolation, evapotranspiration).

3.5 Soil Sample Processing

3.5.1 Total Carbon and Nitrogen Elemental Analysis

The duff layer was sieved to 4 mm with a portion freeze dried, after being kept frozen since acquisition, for analysis of phospholipid-derived fatty acid content (PLFA) and pH. This sieve size was chosen to include the most organic material while reliably removing visibly distinguishable roots in order to reduce their potential interference in PLFA analysis[87]. The remaining fine and coarse fractions of the duff layer, along with the moss/litter and char layers in their entireties, were dried at 40 °C for 3 days and then pulverized for total C and N analysis. The pulverized samples were packed in tin capsules and combusted in a Costech ECS 4010 elemental analyzer, equipped with a 2 m packed chromatographic column for gas separation, to produce values of C and N fraction by sample weight. After every 10 samples, standardized acetanilide (provided by the company Elemental Microanalysis, Okehampton, United Kingdom) was run to calibrate the machine within 1%. Duff layer elemental weight ratios were recalculated by the sum of C or N in its fine and coarse fractions and divided by total sample weight. For each plot, C_R and N_R were multiplied by area-normalized mass of each soil layer, which itself was calculated by multiplying ρ (i.e., bulk density as measured by total soil layer sample weight divided by its volume) by the average measured thickness of that layer, providing C and N values in units of kg m^{-2}. Organic layer area-normalized C and N was calculated by summing those values in each of its included sub-layers and its ρ value was calculated by summing the area-normalized mass of the sub-layers and dividing by their combined depth in meters (producing units of kg m^{-3}). Organic layer C:N was calculated by dividing total organic layer kg C m^{-2} by its kg N m^{-2}. To retain focus on readily measurable forest properties, the effects of soil charring throughout the soil profile were tested as proxied by the kg m^{-2} (i.e., area-normalized total mass) of the sampled pyrogenic char layer alone.

3.5.2 Black Carbon Quantification

Black carbon (BC) was quantified using the chemo-thermal oxidation method at 375 °C (CTO-375)[88,89,90], with adaptation for soil samples[91]. CTO-375 was chosen to isolate an oxidation resistant portion of the PyC pool in order to directly address the effects of fire on C storage. The method also has a relatively low false positive rate, well-tested precision and is practical for applying to a large number of samples[92]. However, by selecting for compounds of low thermolability, the method is expected to give a conservative view of overall C compound change due to the varied heating conditions of wildfire[92]. Although, recent global analysis suggests CTO-375 produces similar PyC concentrations in soils as other common quantification methods[93].

Samples of 15-20 mg were weighed into silver capsules (precombusted at 450 °C). Thermal treatment was performed on the samples in a horizontal tube furnace (Entech EFT30-50) at 375 °C with forced airflow of 250-300 mL min^{-1} for 24 hours. The temperature was continuously monitored with an external probe and ramped slowly to prevent overshoot. After, inorganic carbon was removed by acid fumigation with 12 M hydrochloric acid in a desiccator for four hours. The samples were moistened with 25 μL deionized water before and after fumigation. The samples were dried on a hot plate at 60-70 °C before measurement of the remaining C.

Total C in the remaining sample material was measured using an elemental analyzer (COSTECH ECS4010). The measured remaining C weight was divided by original sample weight to determine the weight ratio of BC (BC:W) within the plot soil layer (given in units of g kg^{-1}). The performance of the elemental analyzer was calibrated every 10 samples using acetanilide (Elemental microanalysis, UK) and compared to measurements of a soil standard (Boden standard, Säntis analytical AG, Switzerland). The detection limit was 1.3 μg C, estimated as the average C response in blank runs plus five times the standard deviation (n = 5). No standard for BC is available, and the BC quantification was evaluated against replicated measurements (n = 5) of reference materials NIST1944 (sediment) and SRM 2795 (diesel soot), with published BC quantification. The measured BC concentrations in the reference materials were 0.73 ± 0.09% for NIST1944 and 67.5 ± 0.9% for SRM 2795, and are within the ranges of published values (NIST1944: 0.8 ± 0.02%, SRM 2795: 68.2 ± 0.9%)[89].

3.5.3 Duff pH Measurement

pH was measured on the < 4 mm freeze dried duff samples using an HI pH-211 meter (Hanna Instruments). 1.0 g of soil was mixed with 20.0 mL of deionized water (resulting in an approximated 1:2.5 volume:volume dilution) and shaken vigorously for at least 1 min. The electrode was immersed in this solution for an additional 1 min, giving stable readings to two decimal places.

3.6 PLFA Processing and Data Handling

Freeze dried soil samples were sent to the Swedish University of Agricultural Sciences location in Umeå, Sweden for processing of PLFA markers. The extraction and methanolysis of the soil PLFA followed the method in Bligh and Dryer[94] as modified by White et al[95]. Resulting fatty acid methyl esters (FAME) were injected into a Trace GC Ultra gas chromatograph (Thermo Fisher Scientific, Bremen, Germany) by means of splitless injection and separated by a 30 m $\times$ 0.25 mm $\times$ 0.25 μm DB-5 column (Agilent Technologies, Santa Clara, CA). The chromatographic conditions were as follows. Injection volume: 1 μL; injection split ratio: 10; injector temperature: 280 °C; carrier flow: 1 mL min^{-1}; temperature gradient: starting temperature 80 °C, hold for 1 min, increase to 155 °C at 20 °C min^{-1}, hold for 0 min, increase to 300 °C at 20 °C min^{-1}, hold 15 min. Samples were subsequently analyzed by an ISQ LT single quadrupole mass spectrometer (Thermo Fisher Scientific, Bremen, Germany). This gave quantitative measures of 24 individual FAME compounds as nmol per g soil sample, as calibrated by an internal standard of methyl nonadecanoate (19:0) provided by Sigma-Aldrich (product number 74208). Instrument stability and retention times were verified using bacterial acid methyl ester (BAME) and Supelco 37 Component FAME mixtures both provided by Sigma-Aldrich (respective product numbers 47080-U and CRM47885).

Total measured PLFA can be suitably used as a metric of living soil microbial biomass due to its tendency not to persist as soil organic matter[87,96,97]. The spectroscopically measured FAME concentrations were utilized as an estimate of relative microbial biomass per mass soil (nmol g^{-1}) across the sampled plots and abbreviated as "MicConc". Total microbial biomass per unit area was calculated by multiplying MicConc by soil organic layer mass (producing units of nmol cm^{-2}) and abbreviated as "MicMass".

Fungal PLFA markers for each plot were considered as the sum of the measured methylated fatty acids 16:1ω5, 18:2ω6,9, 18:1ω9[96,98]. Actinobacteria consisted of 10Me16:0, 10Me17:0, 10Me18:0 markers[96,98]. GN bacteria were the sum of cy17:0, cy19:0, 16:1ω7, 16:1ω9, 17:1ω8, and 18:1ω7[96,98,99]. The GP bacteria were the Actinobacteria marker concentrations plus i14:0, i15:0, a15:0, i16:0, i17:0, and a17:0[99]. General bacteria were the sum of the markers for GP and GN[98]. Because the remaining markers 14:0, 15:0, 16:0, 17:0, 18:0, and 20:0 are not unique to any of these groups[96,100], they were only used in the estimates of total microbial biomass (i.e., MicConc and MicMass).

The F:B ratio was constructed for each plot by dividing the fungal PLFA concentration by the general bacteria. GP:GN was calculated by dividing GP markers by GN. Act:F was formed by dividing Actinobacteria markers by fungal, though excluding 16:1ω5 which is representative of arbuscular mycorrhizal fungi[96], in order to better isolate the relationship between Actinobacteria and saprotrophic fungi (though these 2 markers do not distinguish free-living saprotrophs from ectomycorrhizal fungi[96]). The variable Arb:F was constructed by dividing the arbuscular mycorrhizal fungi FAME concentration by all three fungal markers.

3.7 Resin Capsule Installation, Processing and Data Handling

300 count PST-1 ion-exchange resin capsules were purchased from Unibest (Walla Walla, Washington). During the 2019 field campaign, 3 resin capsules per plot were buried equally spaced radially at about 5 m from the plot center in the organic layer consistently at approximately 2 cm above its interface with the mineral layer below. There they acted to adsorb solvated ions effectively irreversibly, providing a time-integrated view of nutrient mobilization into the soil solution. 277 viable resin capsules were retrieved during a second field campaign approximately 1 year later, with the remaining missing or damaged. The northernmost burnt plot was salvage logged between installation and retrieval, causing major disturbance, and resin capsules from its control pair were not found. Therefore sample size for analyses involving resin capsules and recovering plant communities was reduced to n = 49 for burnt and control plot analyses each, and their differences (n = 50 for all analyses excluding resin capsule and floristics data). While in the field, the capsules were cleaned by shaking vigorously in a sealed vial with several applications of clean deionized water until applied water was clear and free from debris. Capsules were kept refrigerated each in individual plastic bags until sent back to Unibest for processing.

Lab work was managed by Unibest and involved further cleaning with deionized water and then extraction of resin capsule adsorbates individually by rinsing with 2 N HCl at a rate of 1 mL min^{-1} for 50 minutes, resulting in volumetric 50 mL solutions of leachate. Each solution was separately analyzed for concentration of chemical species and given in ppm (mg L^{-1} for mass of target element alone). NH_4 and NO_3 concentrations were determined from aliquots of the extract solutions using flow injection analysis (FIA) and UV/VIS spectroscopy with an FIAlab-2500 (FIAlab Instruments, Seattle, Washington). Concentration of 12 elements (P, K, S, Ca, Na, Fe, Mg, Cu, Zn, Mn, Al, B) were determined using inductively coupled plasma optical emission spectroscopy (ICP-AES) using an Agilent 5110 ICP-OES (Agilent Technologies, Santa Clara, California). This technique is destructive, involving injecting of the extract solution into a high energy plasma, and provided only the concentration of the elements based on their unique spectroscopic signature, not the identity of their resin-adsorbed ionic forms. Resulting ppm values for both characterization methods were matrix matched by identical processing of separate resin capsules which were soaked in 3rd party manufactured standard solutions of common soil ions. This procedure was performed before every 25 samples run and provided an analytical repeatability within $\pm$ 0.5%. The resulting 277 sets of ppm values were averaged per plot providing 49 burnt and 49 paired control values for each chemical species. 3 additional constructed variables were used in analysis. These were iN (inorganic nitrogen), the sum of the NH_4 and NO_3 variables, NH_4:NO_3, the NH_4 variable divided by NO_3 and iN:P, iN divided by the P variable.

3.8 Remotely Derived Data

3.8.1 Standardized Precipitation-Evapotranspiration Index

The shorter term moisture balance of summer 2018 was assessed with the Standardized Precipitation-Evapotranspiration Index (SPEI) due to its observed relationship to fuel drying and fire activity in boreal Eurasia[101,102]. SPEI was calculated over the first 6 months of 2018 at 0.5° spatial resolution within the SPEIBase data source to capture the extended desiccation process leading up to each fire[103]. Due to limited temporal information on 2018 fire activity, common fire weather metrics were unavailable and were instead approximated by summer 2018 anomalies in temperature (ΔMAT) and precipitation (ΔMAP), i.e., the difference in the 2018 June, July, and August average of these values from those during the same months averaged over the period from 1961 to 2017.

3.9 Data Analysis

3.9.1 Variable Construction

3.9.1.1 Paper I

Paper I aimed to establish a potential causal chain of climatic influence on the post-fire restructuring of ecosystem C and N. Utilized variables were therefore temporally categorized to establish their direction of causality as found in Table 3.1.

Table 3.1: Main variables used in Paper I listed and grouped by category. Each category row is assumed to have a potential causal effect on lower rows.

Category	Variables
climate/drainage	MAT, MAP, TEM
prefire organic soil	C, N, C:N, C_R, N_R, bulk density, depth
time-of-fire	SPEI, ΔMAT, ΔMAP, char C, char N
postfire	C loss, N loss

The composition of the different organic material storage compartments were also used in analysis and formulated as in Table 3.2.

3.9.1.2 Paper II

Paper II attempted to explain shifts in BC and BC:C in the organic and mineral layers using MAT, MAP, TEM and the loss of organic layer C due to burning. Control plot BC and BC:C were attempted to be explained by their respective compartment total mass, total C, C:N and plot TEM.

3.9.1.3 Paper III

Paper III aimed to use readily measurable predictor variables (Table 3.3) to explain the PLFA indicators F:B, GP:GN, Act:F and MicMass and all nutrient values from the resin capsules.

3.9.1.4 Paper IV

Paper IV used a set of environmental variables (Table 3.4) to explain the species and functional group patterns of the floristic survey performed in burnt plots during the

Table 3.2: Paper I Compartment composition variables (CCV) categories for ecosystem compartments given in dry weight (kg).

Compartment	Categories
mineral	coarse ($\geq$ 2 mm), fine ($<$ 2 mm)
duff	coarse ($\geq$ 4 mm), fine ($<$ 4 mm)
moss/litter	needles, broad leaves, woody material, moss and lichen
understory	graminoids, forbs, shrubs, pteridophytes
overstory (aboveground)	stem wood, stem bark, living branches, dead branches, stump, needles
overstory (belowground)	coarse roots ($\geq$ 5 cm), fine roots ($<$ 5 cm)

Table 3.3: All climate and forest property predictor variables used in Paper III analysis with units and description of their derivation.

Variable	Unit	Derivation
MAT	°C	1961-2017 averaged mean annual temperature
MAP	mm	1961-2017 averaged mean annual precipitation
TMort	%	Percentage of non-living tree stems plot-wide
pH	–	pH value extracted from duff layer
ρ	kg m^{-3}	Organic layer bulk density
C:N	–	Organic layer total C divided by total N
char	kg m^{-2}	Pyrogenic layer mass (burnt plots only)
C	kg C m^{-2}	Total area-normalized organic layer C

second field campaign. Species richness was calculated simply as the number of plant species within biomass samples per plot. Regrowth rate of the sampled plant communities was calculated as the total dry biomass collected per burnt plot sampled area measured in 2020 and given in units of g m^{-2}.

3.9.2 Statistical Distributions, Confidence Intervals and Percentage Change

Three statistical distributions were formed for sampled variables, one for their control plot values, burnt plot values and another for the values produced by subtracting control plot values individually from those in their paired burnt plot (Δ variable distributions). MAT and MAP (given at 2 km resolution) were identical for each control-burnt plot pair, and so the same values were used within control, burnt and Δ variable analyses. All variable distributions (except MAT and MAP which were only analyzed as a predictor variable) were approximated as normal.

Confidence intervals were marked with the $\pm$ sign and constructed at the 95% level using the formula

$$I = \bar{x} \pm z \cdot \frac{\sigma}{\sqrt{n}} \tag{3.1}$$

Table 3.4: Independent variables used in regression and distance-based redundancy analyses for Paper IV.

Variable	Unit	Derivation
MAT	°C	1961-2017 averaged mean annual temperature
MAP	mm	1961-2017 averaged mean annual precipitation
LiveConifer	$m^2\ ha^{-1}$	Basal area of living conifers
ResOL	cm	Residual organic layer thickness in burnt plots
BurnDepth	cm	Reduction of organic layer thickness due to fire
ρ	$kg\ m^{-3}$	Organic layer bulk density
C:N	–	Organic layer total C divided by total N
pH	–	pH value extracted from the duff layer
iN	ppm	Resin capsule adsorbed NH_4 and NO_3 in organic soil
GP:GN	–	Ratio of gram-positive to gram-negative bacterial PLFA markers
MicConc	$nmol\ g^{-1}$	Concentration of PLFA markers per duff sample mass

where $\bar{x}$ is the sample mean, z is always 1.96 (the critical value for a two-tailed Z-test at α = 0.05), σ is the sample standard deviation and n the sample size. Significance of differences between control and burnt plots was deemed to be when the interval of their Δ variable distributions did not include zero. Coefficients of variation (CV) were calculated as the standard deviation of a variable distribution divided by its mean. Percentage change of variables from burnt to control plots were calculated from the two averaged values derived from the burnt and control plot variable distributions.

3.9.3 Simple and Multiple Regression

Bivariate correlation strength between variable pairs was extracted as the Pearson correlation coefficient (r) from the *scipy.linregress* method from the *SciPy* package[104] in Python 3.

Multiple regression was performed by inputting standardized variables (i.e., converted to Z-scores) to the *OLS* class in the *statsmodels*[105] package using the Python 3 interpreter. The *OLS* class used the ordinary least squares regression approach to predict a single response variable based on linear combinations of predictor variables and gave as an output R^2, R^2_{adj}, Akaike information criteria (AIC), and Bayesian information criteria (BIC) values for the model fit as well as standardized regression coefficients (β) for the explanatory variables.

Forward multiple regression model selection was performed by beginning with the dependent variable producing the highest R^2_{adj} value and adding the variables, one at a time, that most increased this value. Corrected AIC (AICc) was calculated as

$$AICc = AIC + \frac{2k^2 + 2k}{n - k - 1}$$

where k is the number of model parameters and n is the sample size[106]. ΔAICc and ΔBIC values were produced from the difference of the current model from the lowest AICc and BIC in the entire model selection process, respectively.

Backwards multiple regression model selection was performed by removing the explanatory variable with the highest p value until all variables and the total model had p values below 0.05 or only 1 explanatory variable remained.

3.9.4 Canonical Correlation Analysis

Canonical correlation analysis was performed to produce biplots of the multivariate relationships between nutrient and microbial datasets using the *CCorA* class from *vegan*. Significance was extracted from the model object using a permutational (n = 1000) F-test of Pillai's trace. Canonical correlation coefficients were extracted from the model object for the 1st axes of each dataset and R^2_{adj} values were derived from the object's internal calls to the *vegan rda* class.

3.9.5 Redundancy Analysis

Redundancy analysis (RDA) was performed by entering normalized (i.e., converted to Z-scores) datasets using the *rda* class in the R package *vegan*[107], outputting R^2 and R^2_{adj} for each model. Model selection was performed to drop explanatory variables that did not contribute to increasing R^2_{adj} through the usage of the function *ordi2step* within the *vegan* R package. Overall model and per-axis significance was calculated using 1000 permutations in the *anova* function in the R *vegan* package and deemed significant when the produced p value was less than 0.05. The RDA results were displayed as triplots across the two axes of largest explanatory power using the fitted y values (so-called "lc scores"). Canonical coefficients for the explanatory variables were extracted directly from the *rda* object.

Distance-based redundancy analysis (db-RDA) was performed by transforming dependent variables into principal coordinates using the Bray-Curtis dissimilarity and then performing RDA as above, though using the class *capscale* in the R package *vegan*.

Variance partitioning was executed by segmenting explanatory variables into groups and calculating their individual and shared explained variance in terms of R^2_{adj} using the *varpart* function in the R package *vegan*.

Chapter 4

Results and Discussion

4.1 Paper I: Climatic variation drives loss and restructuring of carbon and nitrogen in boreal forest wildfire

Measuring atmospheric emissions of carbon (C) due to burning has been a central focus of boreal wildfire research since the late 20th century. This can be largely attributed to an enhanced awareness of their positive feedbacks with climate change[108], improved ability to upscale results with advancements in remote sensing[34,109], and mounting concern for public health related to air and water quality[110,111,112]. Wildfire activity can now be mapped to 20 m resolution using satellite measurements largely based on determining changes in surface reflectivity due to vegetation removal[113]. These areas can be multiplied by area-normalized emission estimates to determine ecosystem change in C. While burn area mapping is more straightforward (though still presenting an ever-improving set of complicated algorithms), estimating areal emission rates entails a variety of less-direct approximation methods. Of these, remotely observable heat radiation or particulate emissions are often used to estimate yearly C emissions[114,115,116,117,118]. Though, these must be found to correlate with more direct measurement of change in ecosystem C under a process of ground truthing.

Due to the small percentages of annual burnt area and unpredictable emergence of wildfire, field measurements in boreal forests are almost always challenged by a scarcity of information regarding a forest's prefire state. Prefire overstory biomass can be estimated by allometric equations, usually calculated from measurements of stem diameter, with combustion only roughly estimated via visual assessment of the extent of blackening of the components of the tree body[75]. Soil consumption can be estimated by comparing postfire depth with indicators of its original height such as adventitious tree roots (when present), with original C volumetric density calibrated to that in spatially proximal unburnt stands[75]. Though without such indicators, prefire soil properties have to be estimated entirely via matched unburnt control plots.

Random error in plot pair matching can be mitigated by averaging high measurement replication dispersed inside and outside a burn scar. Although, this process can leave systematic error undetected, potentially over or underestimating wildfire emissions due to burnt forests containing different amounts of prefire soil C than those left unburnt. That is, all C emission measurements in the field are, to unknown extent, partly to near-fully determined by systematic differences in estimated and actual prefire C. Of particular concern is the propagation of this error into analysis of the drivers of C emissions, where variation in reconstructed prefire structure may be linked to systematic bias rather than actual emissions. To reduce this risk, a large signal to noise ratio can be implemented by stretching and matching plot pairs across extensive variation of the influences that affect C accumulation such as site drainage and climate. While this may reduce emission estimate constraint, it enhances the ability of a study to robustly explain the factors influencing emission variability.

An unknown amount of bias is also introduced into traditional wildfire study approaches due to spatial autocorrelation of sample replication in single or closely grouped burn scars[64]. Stand-structure derived drivers of fire severity interact with local fire weather as well as the amount of energy that managed to build up in the firefront and transferred to forest ahead. For example, saturation of built up energy in high intensity wildfire may override otherwise important controls of fuel arrangement, weather and moisture conditions on C emissions[119]. A goal of boreal wildfire study should not only be to isolate drivers of its severity, but to understand when certain sets of them are important. This is especially salient when considering the broad range of forest structure that can be constructed under the influence of current and future climatic conditions. Therefore, expanded sampling of the extensive variation of forest structure and burn dynamics in understudied boreal regions, with methodological tuning designed to expose and reduce bias in the understanding of the influence of climate on wildfire elemental restructuring is crucial for better understanding the connection of boreal forests to future global C cycling.

Paper I utilized the 100 plot network (50 burnt, 50 paired controls) to determine the direct and forest structure mediated controls of climate on boreal wildfire emissions. Across all burnt plots, negligible canopy blackening was found along with insignificant differences in mineral layer soil C, leading to assumptions that the near entirety of emissions came from the organic soil layer. Averaged across the plots, C loss was significant (0.815 ± 0.652 kg C m^2), and approximately a quarter of that typical of more intense North American boreal wildfire (3.3 kg C m^2)[75,119]. Mean annual pre-

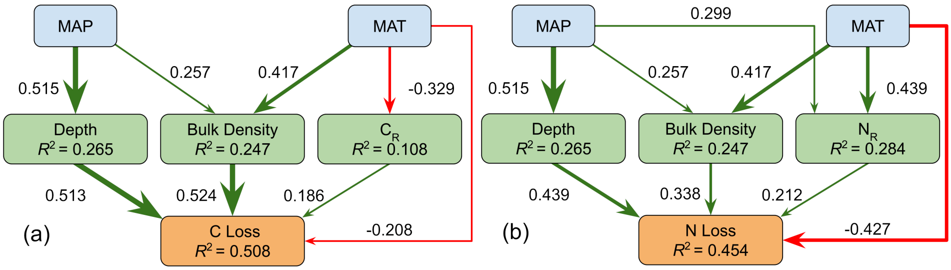

Figure 4.1: Diagram of proposed pathways for the effects of MAP and MAT on C (a) and N (b) loss. Non-climate variables regard the organic layer. Each variable node is labeled with the R^2 from simple or multiple regression using explanatory variables represented by all incoming arrows. Arrows are labeled by and sized in proportion to the magnitude of their standardized regression coefficients and are significant (p < 0.05). Green arrows represent positive relationships while red represent negative relationships. Omitted for simplicity are direct correlations between bulk density to C_R (p = 0.010, r = 0.356) and depth to N_R (p = 0.010, r = -0.363).

cipitation (MAP) had strong controls on organic layer depth while mean annual temperature (MAT) stronger controlled its bulk density and negatively influenced the carbon mass fraction (C_R), as seen in Figure 4.1a. Prefire estimated organic C was the strongest predictor of its loss during burning. Higher prefire organic layer C:N augmented C loss, while the collection of heat-affected fuel as char suppressed it (Figure 4.2a). Together, these results signify that climate has a strong fuel conditioning effect in terms of its total amount, structure (depth and density), and elemental composition (likely largely a product of litter input, microbial growth and decomposition state) that together influence the relative emissions of C.

Despite its recognized role as a limiting nutrient in boreal systems, the release of nitrogen (N) during wildfire burning is seldom measured alongside C. This is likely due to assumptions that N is emitted at similar rates as C, as has been observed in high intensity fire in interior Alaska[75]. Yet analysis of pyrogenic soil layers in Eurasian boreal forests has shown a decrease in C:N relative to prefire material[61]. The current study observed an insignificant loss of N from the soil as a whole, but found it to concentrate in a highly nitrogenous layer of char, reducing the organic layer C:N from a prefire average of 47.68 to 38.22. N loss was strongest driven by prefire organic layer N, and had strong mitigating effects from MAT and its concentration in a layer of low C:N char (Figure 4.2b). This conservation effect for N has major biogeochemical implications and regional differences in thermolability of this element may be fundamentally responsible for altered ecosystem recovery trajectories. Namely, N fertilization can both enhance soil decomposition rates and allow its greater uptake by plant life[41], potentially extending net C emissions beyond the time of burning and initiate overstory dominance shifts to broadleaf trees[52].

Paper I demonstrated the importance of climate in determining the prefire structure of fuel that controls the emissions of C and N during wildfire and their proportional

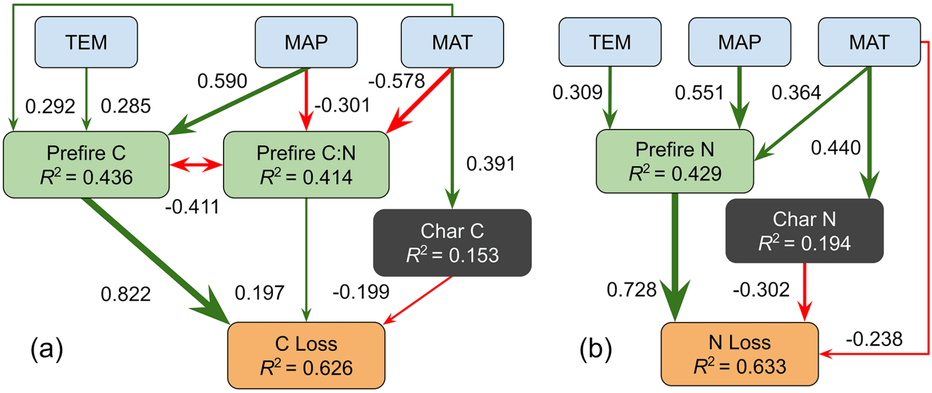

Figure 4.2: Path diagrams for C (a) and N (b) loss including char and C:N variables. Prefire C, N, and C:N as well as losses of C and N are regarding the organic layer. Each variable node is labeled with the R^2 from simple or multiple regression using explanatory variables represented by all incoming arrows. Arrows are labeled by and sized in proportion to the magnitude of their standardized regression coefficients and are significant. Green arrows represent positive relationships while red represent negative relationships.

reorganization into pyrogenic soil compartments. This asserts an importance of inciting more detailed standards for soil measurement that include the shifted densities and elemental ratios of its varied compartments in order to more accurately predict wildfire emissions and soil restructuring. Despite careful plot pair matching extending over wide gradients of the variables that control fuel accumulation and structure, measurement of N made clear the impact of bias on emissions estimates. From the organic layer, N loss was centered near 0, yet it formed strong correlation ($p < 0.001$, $r = 0.653$) with prefire N, signaling a desirably high signal to noise ratio of its variation across climate but a systematic error that underestimated its averaged removal. Furthermore, virtually no canopy burning was observed, with near-complete understory removal and surface blackening, meaning there was little remotely observable variation of fire impact to correlate to the burning underground. Therefore, this study demonstrates the potential for widespread inaccuracy in wildfire field sampling methodology as well as the danger in projection of remote methods outside of burn dynamics for which they are calibrated. More insight is needed into the factors that determine fuel structure and its susceptibility to combustion in order to more accurately measure and model emissions from boreal ground fire.

4.2 Paper II: Mineral Soils Are an Important Intermediate Storage Pool of Black Carbon in Fennoscandian Boreal Forests

Field measurements that estimate wildfire emissions are usually performed at 1 year postfire in order to allow the forests to cool and stabilize to an initial state under which secondary succession begins. While this might be a good strategy in the context of ecological study, it makes dubious the common and often unstated assumption that the majority of estimated emissions by this stage were atmospheric. Wildfire can mechanically and chemically restructure ecosystem material, immediately stimulating its mobilization through the surrounding land and waterways, providing for escape from delayed postfire measurement[120,121]. Nutrient pulses to aquatic systems are often observed within the first years after nearby fire[122]. Although, pyrogenic carbon (PyC) tends to form consistent ratios with the larger dissolved organic C pool in rivers over time, suggesting that the landscape buffers its expulsions from the watershed between fire seasons[123]. While PyC production and sedimentation in limnic and ocean sediment is beginning to be quantified globally, little is known about the drivers of its transport from the fast to slow C cycle, and its interactions and degradation processes along the way[42,124].

Varied parent material and burn conditions provide for a boundless diversity of PyC composition[38,39,125,126]. This diversity interacts with the structure and metabolic strategy of its containing ecosystem to determine its residence time. For example, irregular PyC structure may hinder rapid enzymatic decomposition, extending its lifetime beyond more labile ecosystem C. However, addition of these refractory compounds to the soil has the potential to enhance decomposition rates through increasing soil specific surface area and cation exchange capacity providing habitat and reservoirs of water and nutrient that stimulate biotic activity. In contrast, more mobile PyC fractions can escape areas of high degradation altogether at rates determined by their interaction with the structure and hydrology of the soil[121]. Therefore, it is important to derive understanding of how different PyC features connect to their environmental conditions to more fully determine the impact of wildfire on local, regional and global C cycles.

Many techniques exist for quantifying PyC in forest soils, each isolating only a fraction of its total diversity and providing varied levels of detail on its chemical and structural form. While production rates of many of these fractions can be predicted under controlled fuel and burn conditions, little knowledge is available to predict covariation patterns of their synthesis under natural wildfire conditions[127]. This means that any correlation found between production of a single PyC fraction and ecosystem function

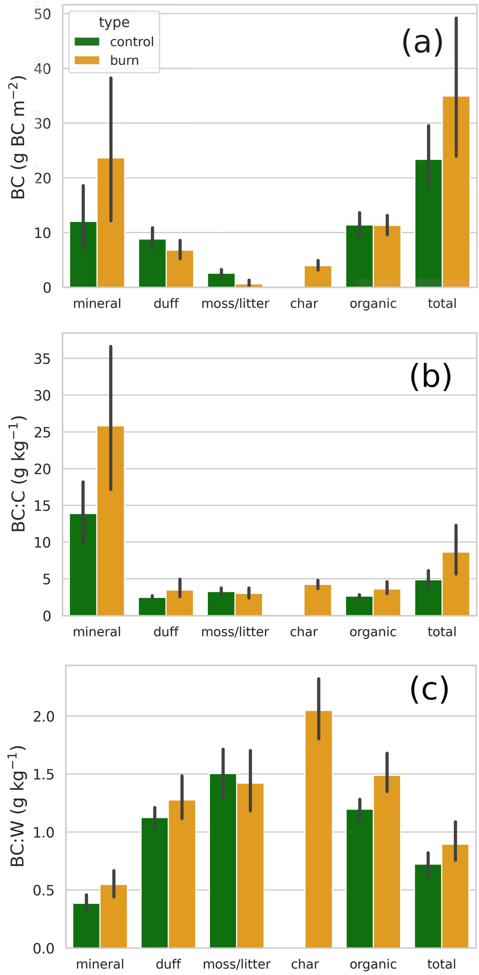

Figure 4.3: Mean BC stocks (a), BC:C (b), and BC:W (c) between burnt and control plots amongst forest soil compartments. The organic layer is considered the grouping of the duff, moss/litter, and char layers while the total category is the grouping of the organic and mineral soil layers. Error bars are the bootstrapped 95% confidence interval of the mean (n = 1000).

can be due to confounding with drivers of its production or covarying presence of other PyC fractions. While in practice these statistical caveats are difficult to fully escape, they can both be mitigated and better understood through careful selection of investigative methodology.

Paper I found climate to be an important factor in determining the rate of production of pyrogenic layers on the forest floor. Yet questions remained regarding how climate and wildfire altered the degradability of the soil throughout its compartments. To answer this question the chemo-thermal oxidation at 375 °C (CTO-375) method was

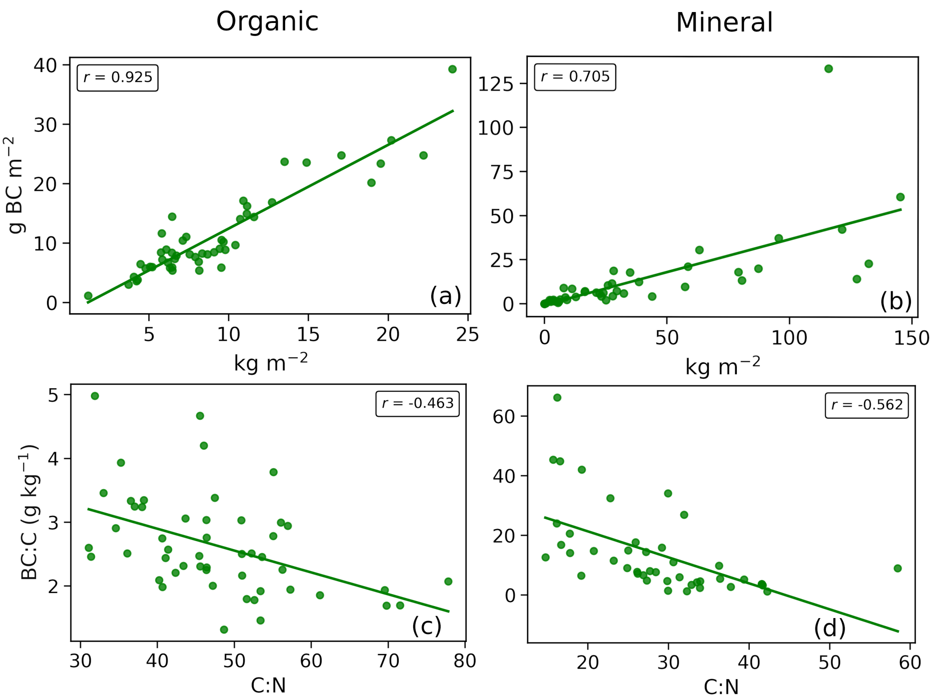

Figure 4.4: Simple regression charts for the 50 control plots regarding organic layer total BC against its layer mass (a), mineral layer total BC against its layer mass (b), organic layer BC:C against its C:N (c), and mineral layer total BC against its C:N (d). All regressions have $p < 0.001$.

used across the sampled soil compartments of the 100 plots. CTO-375 exposes soil material to 375 °C, followed by removal of inorganic C via fumigation, and measures C percentage in the remaining sample[128]. This method gives a more simple and direct measurement of a material's intrinsic thermo-oxidative lability, when compared to techniques that only indirectly estimate this property through visual or chromatographic separation followed by chemical characterization of broadly defined patterns of chemical functional groups. Thus, CTO-375 has the potential to better isolate the burn conditions that produce and distribute this particularly recalcitrant PyC fraction, here-called black carbon (BC), and thereby also serve as an indicator of fire severity and its impact on overall soil degradability.

Surprisingly, BC addition to burnt soils was not correlated to climate (MAT, MAP), site drainage (TEM), drought extent (SPEI) or fire severity (loss of C). Though it was found that fire did not significantly shift total BC in the organic soil layers, but approximately doubled it in the mineral layer (Figure 4.3), providing a total soil increase of 11.6 ± 10.4 g BC m^2. Because mineral soils tend to receive lower heating during wildfire compared to the organic layers above[129], it was assumed that mineral layer additions were due to a flooding of BC released from above. The strongest determinant of BC storage in control plot organic ($p < 0.001$, $r = 0.925$) and mineral ($p < 0.001$, $r = 0.705$) layers was their total respective mass. The ratio of BC to C in the organic ($p < 0.001$, $r = -0.463$) and mineral ($p < 0.001$, $r = -0.562$) correlated negatively with their C:N (Figure 4.4). Together these results suggest that the sampled PyC fraction is both highly mobile and degradation resistant, and depends upon binding to stationary soil material to remain in the profile for extended periods. Furthermore, it was proposed that the mineral soils are an important intermediate storage pool of C that buffers the production of BC and its transport to neighboring systems, which will become increasingly important for the protection of C from mineralization in a future of increased fire activity and decomposition rates in organic soils (Figure 4.5).

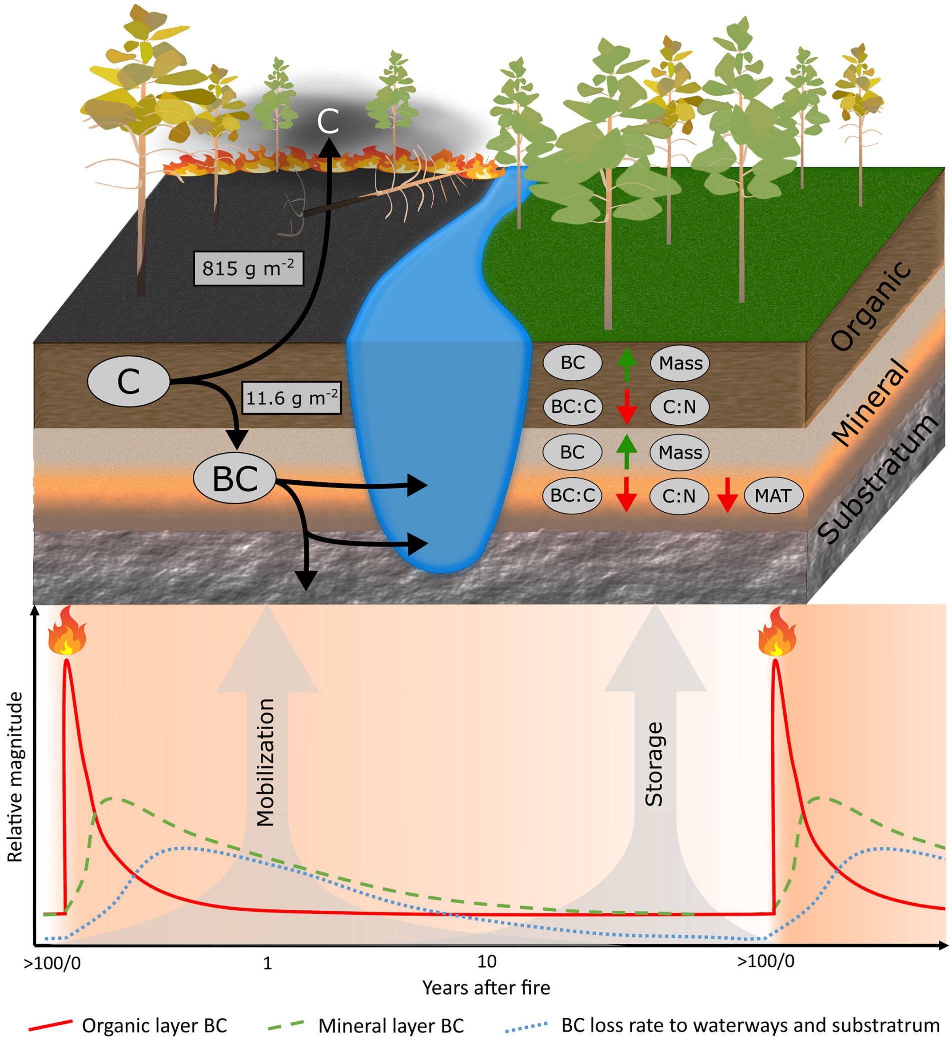

Figure 4.5: Conceptual diagram of carbon (C) and black carbon (BC) cycling proposed by the results of Paper II. The landscape diagram depicts temporal division of early postfire BC synthesis and mobilization (left) and late postfire BC storage patterns (right). Measuring the 50 plot pairs, fire was estimated to release an average of 815 g C m^{-2} from the soil as a whole while adding 11.6 g BC m^{-2} to the mineral layer which is assumed to have percolated from the organic layer above over the 1 year postfire period. This high mobility of BC and its strong correlation to total soil layer mass in late postfire control plots suggest this fraction of the pyrogenic C spectrum depends largely on adsorption sites to remain within the soil profile. Negative correlation of soil layer BC:C to the C to nitrogen ratio (C:N) suggests BC is relatively resistant to decomposition processes compared to the larger C pool. Mineral layer BC:C has an additional negative effect of mean annual temperature. This resistance, along with low overall decomposition in mineral layers and the measured approximate doubling of its BC stocks in recently burnt forests, indicates a large portion of the BC additions are lost from this layer to waterways and deeper subsoils over the fire interval. The figure's lower panel charts a hypothetical time series of BC transport, where fire induced increases of BC in the organic layer are largely released within 1 year to lower subsoils. Mineral layer BC stocks are released more gradually to waterways and the substratum until stabilizing at an amount proportional to its total mass before the return of fire.

4.3 Paper III: Climate and forest properties explain wildfire impact on microbial community and nutrient mobilization in boreal soil

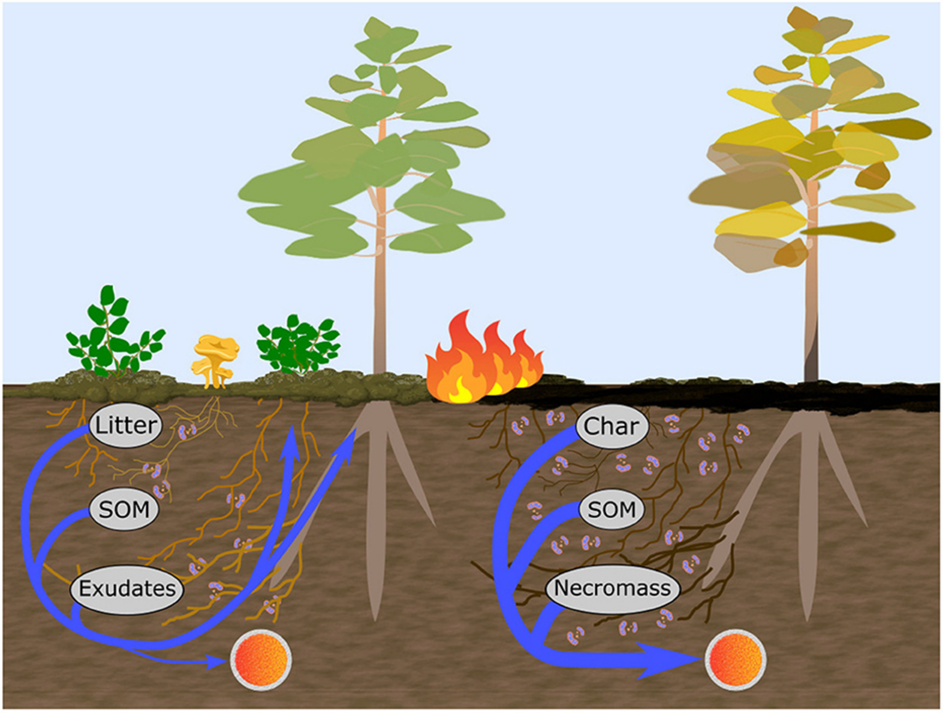

Figure 4.6: Conceptual diagram motivating Paper III hypotheses. Unburnt soils (left) receive inputs of plant-derived litter and root exudates containing labile C. Microbial C copiotrophy and plant nutrient demand promotes retention and/or immediate reuptake of relatively limited N within microbial and plant biomass during processing of organic matter, hindering its net mobilization as measured by ionic-resin capsules (orange spheres) installed at the bottom of the organic soil layer. Burning (right) typically completely removes understory vegetation and increases stand overstory mortality, removing a large portion of fresh C inputs and leaving behind charred material, residual heat-altered soil organic matter (SOM) and necromass (darkened root and mycorrhizal webs to the right). This restriction to a more refractory C pool at 1 year post-fire was expected to induce a wider spread C limitation in the soil thereby increasing dominance of oligotrophic microbial C metabolism (e.g., via increased gram-positive bacteria, right image) which enhances net mobilization of excess N and other nutrients (arrows) found in processed organic matter.

Paper I found substantial influence of both climate and wildfire on the restructuring of the organic soil layer and mortality of vegetation. These impacts can further influence the soil microbial community and associated nutrient cycling in the subsequent years of forest recovery. Specifically, the reduction in primary production leaves C to be sourced to a greater extent from residual heat-altered, high-N soil organic matter than plant litter and root exudates, providing for the proliferation of nutrient-mobilizing oligotrophic saprotrophy (Figure 4.6). Paper III aimed to quantitatively measure the

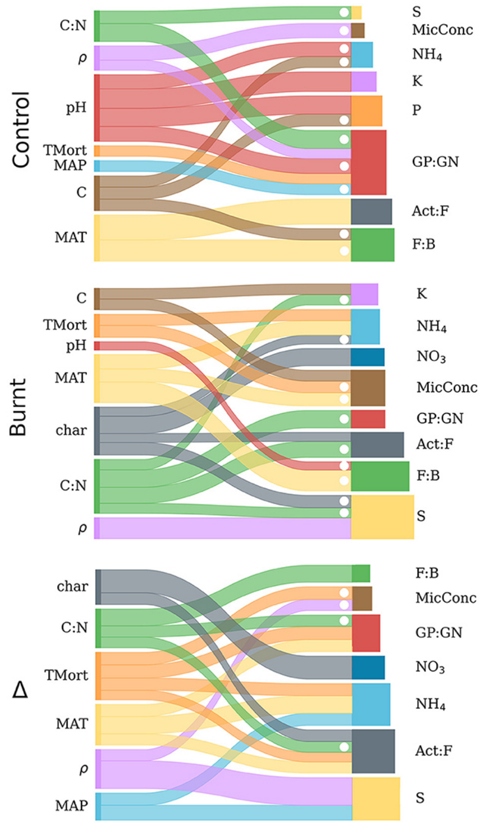

Figure 4.7: Sankey diagrams representing the backwards-selected multiple regression results from control, burnt and Δ variable distributions. For each of the 3 graphs, explanatory variables are listed on the left and connected by ribbons to the dependent variables they predict (right). Ribbon width is scaled to the magnitude of the standardized regression coefficient from its corresponding independent variable (within each graph, but not across graphs), and dotted when this value was negative. The bars on the right sides of the graphs are scaled horizontally to the R^2 values derived from multiple regression for each independent variable and are proportional across all graphs.

impacts of climate and readily measurable forest structure on metabolic shifts in the soil as expressed through microbial community configuration and its mobilization of nutrient. This was accomplished using multiple statistical approaches to compare the 50 control plots, 50 burnt plots, and their paired differences (Δ values).

In the control plots, nutrient cycles were more closed than their burnt counterparts, with the mobilization of the macronutrients NH4, P, and K to resin capsules being determined strongest by organic layer pH (Figure 4.7) with no significant connection to the microbial community as sampled (Figure 4.8). Wildfire significantly opened forest nutrient cycles, increasing resin adsorption of NH4 (39.1%), NO3 (438.3%), P (349.7%), K (36.8%), and S (56.9%). Further, the control of pH was released, leaving the mobilization of elements to be greater determined by climate, forest structure and

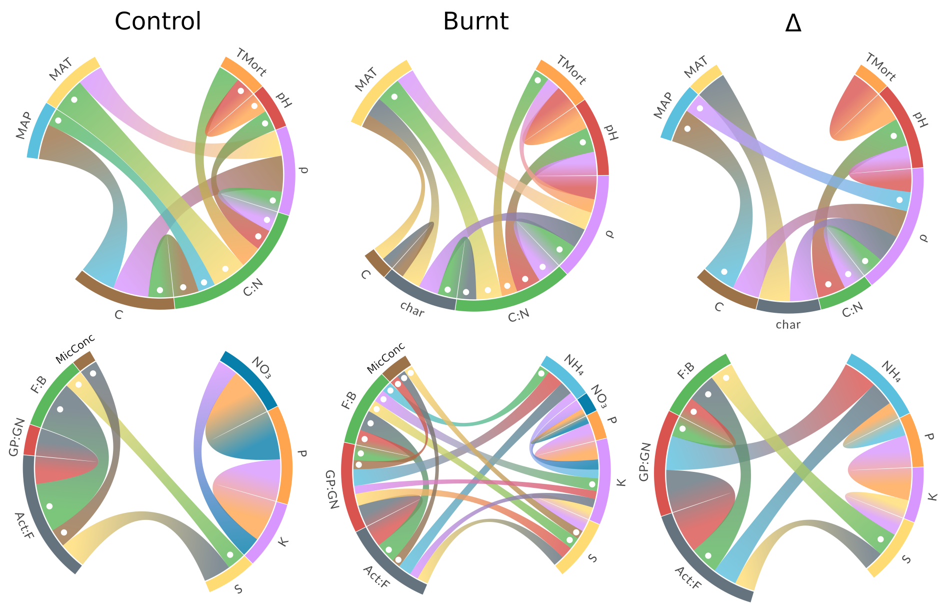

Figure 4.8: Chord diagrams of significant ($p < 0.05$) bivariate correlations between climate and forest properties (top row) and microbe and nutrient variables (bottom row). Ribbon thickness is scaled within each diagram (but not across diagrams) to Pearson's r with negative values dotted.

the microbial community (Figure 4.7). Microbial biomass concentration (MicConc, PLFA moles per gram soil) dropped by 24.2% in burnt plots along with a 13.9% reduction in F:B but a 28.4% increase in GP:GN and 76.7% increase in Act:F. This shift towards oligotrophic bacterial communities provided for their greater connection to measured nutrients (Figure 4.8). GP:GN in particular was strongly associated with the mobilization of NH4 ($p < 0.001$, $r = 0.630$) in burnt plots.

Variation partitioning in redundancy analysis demonstrated that the control of climate on the microbial community structure and nutrient mobilization increased due to burning (Figure 4.9). This increase was almost entirely mediated by shared variation with altered forest structure. Together, the results of Paper III suggest that future climate change can place controls on the ecosystem restructuring of wildfire that can in turn influence shifts in microbial communities towards oligotrophic nutrient mobilization. These shifts can prime growth of more nutrient-demanding temperate plant species or result in nutrient leaching, dependent on the establishment patterns of vegetation post fire.

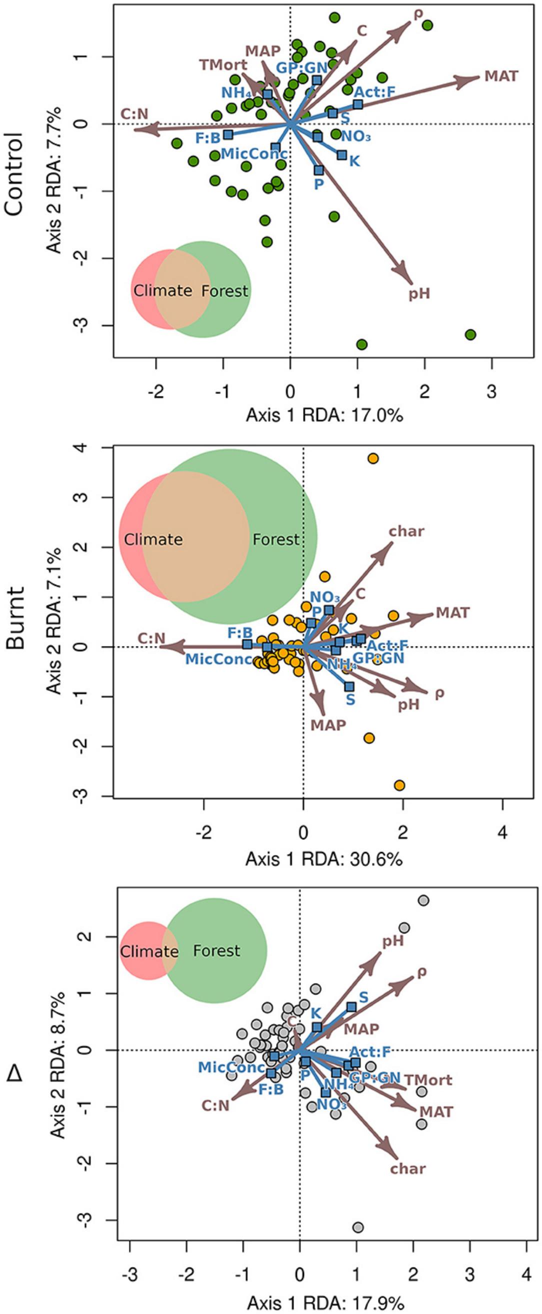

Figure 4.9: Redundancy analysis triplots with explanatory vectors (arrows) scaled by 3 for legibility. Predicted variables are marked by vectors ending in blue squares and plot scores by circles. Variance partitioning is visualized for each chart with relative area of climate (MAT, MAP), forest (all other explanatory variables), and their overlap proportioned across plots to their magnitude of R^2_{adj} for control (climate: 0.041, forest: 0.098, shared: 0.082, total: 0.221), burnt (climate: 0.033, forest: 0.181, shared: 0.153, total: 368), and Δ (climate: 0.053, forest: 0.201, shared: 0.013, total: 267) values.

4.4 Paper IV: Plant biodiversity limits carbon recapture after wildfire in warming boreal forests

Paper III mapped out the synergistic role of climate and wildfire in providing for a fertilization effect in post fire soils. Paper IV aimed to investigate the patterns and extent by which recovering vegetation interact with postfire resource availability and ecosystem structure.

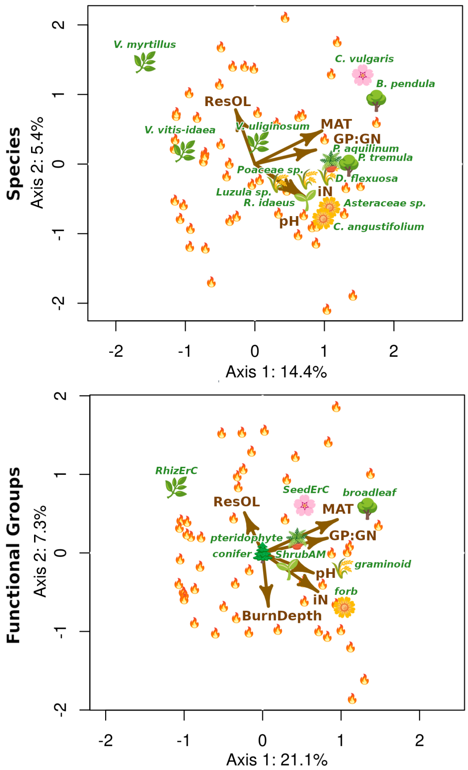

Figure 4.10: Distance-based redundancy analysis explaining sampled plant species (upper panel, R^2 = 0.300, R^2_{adj} = 0.219) and functional groups (lower panel, R^2 = 0.427, R^2_{adj} = 0.345). All displayed axes are significant ($p <$ 0.05). Species scores in the upper panel were doubled to improve legibility.

Climate change and associated amplification of wildfire activity can provide for the shifting of conifer forests to those dominated by deciduous broadleaf trees in boreal North America[58]. This process occurs mostly readily in stand replacing wildfire that removes thick organic soil layers known to inhibit sprouting of broadleaf species from seed. Stand conversion is accelerated by the prefire presence of broadleaf trees providing material for both abiotic resprouting and local sources of seed, forming a positive feedback of propagule pressure and broadleaf dominance in postfire recovery[51]. Seed addition experiments have demonstrated that this increased propagule pressure can even overcome the broadleaf sprouting inhibition placed by residual organic layers and that regrowth in warming high latitude systems in particular is hindered by novel species introduction[130,131,132]. Though it has also been shown that living conifers can enact plant-soil feedbacks that inhibit heterospecific germination and may also provide substantial sink of nutrient together reducing colonization by novel species[54]. Furthermore, rhizomatously resprouting ericoid shrubs may provide for suppression of saprotrophic mobilization of N or even direct allelopathy[21,133].

Paper IV compared a set of environmental variables (Table 3.4) to a floristics survey performed in 49 of the sampled burnt plots (the northernmost plot was excluded from the study due to postfire salvage logging). It was found that the surviving conifer overstory placed no restrictions on N mobilization in the soil (p = 0.757), nor did it influence the assembly patterns of plant propagating from the forest floor (Figure 4.10a,b). The residual conifers did however, place constraints on the species richness of sprouting plants along the gradient of MAT (Figure 4.11a). An additional influence of microbial biomass concentration in the soil suggests a replacement of conifer associated microbes with those more supportive of greater plant diversity.

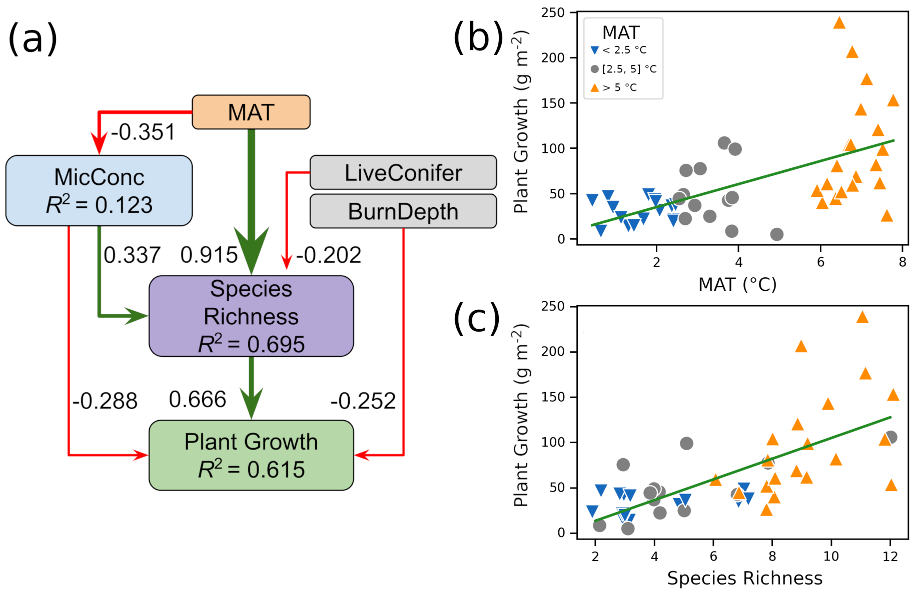

Figure 4.11: Two multiple regression results explaining species richness and plant growth were visualized with incoming arrows labeled, colored and sized according to standardized regressions coefficients of predictor variables (**a**). Significant correlations (p < 0.05) between predictor variables are also labeled. Simple regressions of biomass regrowth on MAT (**b**, r = 0.594) and species richness (**c**, r = 0.699) were plotted. Heteroscedasticity of the MAT regression was reduced by shifting plot plant growth values across the species richness axis. A random number between ±0.2 was added to the species richness values during chart generation to improve legibility.

Under a weakened coniferous influence, rhizomatously resprouting ericoid shrubs appeared to be important for the suppression of nutrient mobilizing bacterial communities and the overall immobilization of N (Figure 4.10b). Though their influence diminished under the warmth of increasing MAT, allowing for increased concentration of bacterial decomposers. Increased MAT and N-mobilizing GP:GN related strongly to broadleaf tree growth (Figure 4.10b). These increases of broadleaf contributions corresponded to an overall increase in biomass regrowth under increasing MAT (Figure 4.11a). Although, the biomass had increased variation at higher temperatures and was better constrained by species richness (Figure 4.11b). Plant growth was additionally negatively constrained by microbial biomass concentrations in the soil and the depth of wildfire burning (Figure 4.11a).

Intermediate wildfire severities (i.e., those that damage the recovery capacity of occupant boreal conifers, but don't burn severely enough to allow rapid broadleaf transition) can provide for forest stagnation of primary productivity. The ability of longer, warmer growing seasons associated with increased MAT to promote plant regrowth are limited by the success of a diversity of warmth-oriented species in establishing through residual inhibitive plant-soils feedbacks. Increasing bacterial decomposition rates under states of limited primary productivity have the potential to extend net C emissions beyond the initial period of wildfire combustion. Further, time-extended study of boreal forest elemental cycling under changing wildfire and climate regimes is imperative for better determining the global land-atmosphere C balance.

Chapter 5

Outlook

A central challenge in the study of Earth is the organization of explanations for its dynamics across analysis scale. Because of their sporadic and sudden impact across the landscape, coordinating field sampling of wildfire events that span their natural variation across a given region is difficult, tending to restrict detailed, on-site study to single burns or burn complexes. While recent advances have been made in understanding biogeochemical cycling within single burn scars, spatially restricted sampling can leave hidden the importance of environmental variation that emerges only over larger areas of land. This thesis provides one of the most comprehensive landscape studies of boreal wildfire, finding climate to be an important factor in shaping the activity and impact of wildfire burning. Furthermore, it demonstrates that microbial community composition is particularly important for the cycling of elements in the postfire environment and can be predicted smoothly across broad ranges of burn severity and forest structure. These communities appear to organize quickly under their associated climate and interact with more slowly assembling plant communities to control the flow of carbon and nutrients within burnt forests.

Differential response of aboveground and belowground forest subsystems to shifting climate and wildfire regimes can complicate prediction of future forest dynamics via their reconnection into novel, unstudied ecosystem configurations. Understanding of processes occurring within individual burn scars is therefore likely to increasingly demand the ability to predict the identity and quantity of biotic inputs from the surrounding landscape under varied states of disequilibrium with concurrent climate. A central demonstration of this thesis is the need to further develop knowledge of wildfire processes that crosses spatial scale in order to improve regional projections of future boreal forest function. Though this predictive power must be supported by environmental monitoring of the continuous reorganization of landscape structure under a currently rapid rate of climatic change. Validating the power of quick, easily-interpretable and low-cost field sampling that allows for monitoring to pace rates of forest change was thus a major goal of the current research effort. Repetition and development of these approaches are encouraged in order to provide more detailed quantification of important elemental and genetic fluxes across the larger expanse of boreal forests throughout the coming future.

The early patterns of natural ecosystem reconnection explored in this thesis also give rise to many uncertainties regarding their effects on subsequent implementation of management strategy designed under previous climatic conditions. These uncertainties are especially great when considering the substantial observed shifts in below-ground communities due to warmth and burning which may limit the growth capabilities of the previously dominant, economically viable conifer overstory. More time-sensitive treatment of boreal forests as complex socioeconomic systems will be important for accurate prediction of future biogeochemical cycling across the boreal region under continued global change. This effort may find climate gradients in particular, such as the one examined in thesis, to be a crucial tool in establishing the boundaries within which natural and anthropogenic processes can operate under fundamental energetic and hydrological inputs, forming a space by which to constrain development of understanding of their interactions.

The pioneers of our understanding of the natural world faced its vastness in awe of its indestructible grandeur. Yet now we are left to rediscover it in its vulnerability. Though we are sure to always be reminded of its tenacity. Life just keeps going, and we have much to learn.

References

[1] A Dalgarno. Molecular processes in the early universe. *Journal of Physics: Conference Series*, 4(1):10, jan 2005. doi: 10.1088/1742-6596/4/1/002. URL https://dx.doi.org/10.1088/1742-6596/4/1/002.

[2] Richard H. Cyburt, Brian D. Fields, Keith A. Olive, and Tsung-Han Yeh. Big bang nucleosynthesis: Present status. *Rev. Mod. Phys.*, 88:015004, Feb 2016. doi: 10.1103/RevModPhys.88.015004. URL https://link.aps.org/doi/10.1103/RevModPhys.88.015004.

[3] Lauren V Jones. *Guide to the Universe: Stars and Galaxies*. Bloomsbury Publishing USA, 2009.

[4] Audrey Bouvier and Meenakshi Wadhwa. The age of the solar system redefined by the oldest pb–pb age of a meteoritic inclusion. *Nature geoscience*, 3(9):637–641, 2010.

[5] A. P. Boss and R. H. Durisen. Chondrule-forming shock fronts in the solar nebula: A possible unified scenario for planet and chondrite formation. *The Astrophysical Journal*, 621(2):L137, feb 2005. doi: 10.1086/429160. URL https://dx.doi.org/10.1086/429160.

[6] George W Wetherill. Formation of the earth. *Annual Review of Earth and Planetary Sciences*, 18 (1):205–256, 1990.

[7] Yutaka Abe and Takafumi Matsui. Early evolution of the earth: Accretion, atmosphere formation, and thermal history. *Journal of Geophysical Research: Solid Earth*, 91(B13):E291–E302, 1986. doi: https://doi.org/10.1029/JB091iB13p0E291. URL https://agupubs.onlinelibrary.wiley.com/doi/abs/10.1029/JB091iB13p0E291.

[8] Paul J. Tackley. Self-consistent generation of tectonic plates in time-dependent, three-dimensional mantle convection simulations. *Geochemistry, Geophysics, Geosystems*, 1(8), 2000. doi: https://doi.org/10.1029/2000GC000036. URL https://agupubs.onlinelibrary.wiley.com/doi/abs/10.1029/2000GC000036.

[9] Dominic Papineau. Mineral Environments on the Earliest Earth. *Elements*, 6(1):25–30, 02 2010. ISSN 1811-5209. doi: 10.2113/gselements.6.1.25. URL https://doi.org/10.2113/gselements.6.1.25.

[10] James C. G. Walker, P. B. Hays, and J. F. Kasting. A negative feedback mechanism for the long-term stabilization of earth's surface temperature. *Journal of Geophysical Research: Oceans*, 86(C10): 9776–9782, 1981. doi: https://doi.org/10.1029/JC086iC10p09776. URL https://agupubs.onlinelibrary.wiley.com/doi/abs/10.1029/JC086iC10p09776.

[11] Thomas G. Huntington. Evidence for intensification of the global water cycle: Review and synthesis. *Journal of Hydrology*, 319(1):83–95, 2006. ISSN 0022-1694. doi: https://doi.org/10.1016/

j.jhydrol.2005.07.003. URL https://www.sciencedirect.com/science/article/pii/S0022169405003215.

[12] James Attwater and Philipp Holliger. A synthetic approach to abiogenesis. *Nature methods*, 11(5): 495–498, 2014.

[13] Daniel Segré, Dafna Ben-Eli, David W Deamer, and Doron Lancet. The lipid world. *Origins of Life and Evolution of the Biosphere*, 31:119–145, 2001.

[14] Anthonie WJ Muller and Dirk Schulze-Makuch. Thermal energy and the origin of life. *Origins of Life and Evolution of Biospheres*, 36:177–189, 2006.

[15] William F Martin, Donald A Bryant, and J Thomas Beatty. A physiological perspective on the origin and evolution of photosynthesis. *FEMS Microbiology Reviews*, 42(2):205–231, 11 2017. ISSN 0168-6445. doi: 10.1093/femsre/fux056. URL https://doi.org/10.1093/femsre/fux056.

[16] Roberto Ligrone and Roberto Ligrone. The great oxygenation event. *Biological Innovations that Built the World: A Four-billion-year Journey through Life and Earth History*, pages 129–154, 2019.

[17] John M Archibald. Endosymbiosis and eukaryotic cell evolution. *Current Biology*, 25(19):R911–R921, 2015.

[18] Daniel S Heckman, David M Geiser, Brooke R Eidell, Rebecca L Stauffer, Natalie L Kardos, and S Blair Hedges. Molecular evidence for the early colonization of land by fungi and plants. *science*, 293(5532):1129–1133, 2001.

[19] Paul Kenrick. Turning over a new leaf. *Nature*, 410(6826):309–310, 2001.

[20] Camille Puginier, Jean Keller, and Pierre-Marc Delaux. Plant–microbe interactions that have impacted plant terrestrializations. *Plant Physiology*, 190(1):72–84, 06 2022. ISSN 0032-0889. doi: 10.1093/plphys/kiac258. URL https://doi.org/10.1093/plphys/kiac258.

[21] Elisabeth B. Ward, Marlyse C. Duguid, Sara E. Kuebbing, James C. Lendemer, and Mark A. Bradford. The functional role of ericoid mycorrhizal plants and fungi on carbon and nitrogen dynamics in forests. *New Phytologist*, 235(5):1701–1718, 2022. doi: https://doi.org/10.1111/nph.18307. URL https://nph.onlinelibrary.wiley.com/doi/abs/10.1111/nph.18307.

[22] Loredano Pollegioni, Fabio Tonin, and Elena Rosini. Lignin-degrading enzymes. *The FEBS Journal*, 282(7):1190–1213, 2015. doi: https://doi.org/10.1111/febs.13224. URL https://febs.onlinelibrary.wiley.com/doi/abs/10.1111/febs.13224.

[23] Philippe Gerrienne, Patricia G. Gensel, Christine Strullu-Derrien, Hubert Lardeux, Philippe Steemans, and Cyrille Prestianni. A simple type of wood in two early devonian plants. *Science*, 333 (6044):837–837, 2011. doi: 10.1126/science.1208882. URL https://www.science.org/doi/abs/10.1126/science.1208882.

[24] Carl J. Douglas. Phenylpropanoid metabolism and lignin biosynthesis: from weeds to trees. *Trends in Plant Science*, 1(6):171–178, 1996. ISSN 1360-1385. doi: https://doi.org/10.1016/1360-1385(96)10019-4. URL https://www.sciencedirect.com/science/article/pii/1360138596100194.

[25] Robert F. Stallard. Terrestrial sedimentation and the carbon cycle: Coupling weathering and erosion to carbon burial. *Global Biogeochemical Cycles*, 12(2):231–257, 1998. doi: https://doi.org/10.1029/98GB00741. URL https://agupubs.onlinelibrary.wiley.com/doi/abs/10.1029/98GB00741.

[26] Heinrich D Holland. The oxygenation of the atmosphere and oceans. *Philosophical Transactions*

of the Royal Society B: Biological Sciences, 361(1470):903–915, 2006. doi: 10.1098/rstb.2006.1838. URL https://royalsocietypublishing.org/doi/abs/10.1098/rstb.2006.1838.

[27] N. J. Butterfield. Oxygen, animals and oceanic ventilation: an alternative view. *Geobiology*, 7(1):1–7, 2009. doi: https://doi.org/10.1111/j.1472-4669.2009.00188.x. URL https://onlinelibrary.wiley.com/doi/abs/10.1111/j.1472-4669.2009.00188.x.

[28] Klaus Schmidt-Rohr. Oxygen is the high-energy molecule powering complex multicellular life: Fundamental corrections to traditional bioenergetics. *ACS Omega*, 5(5):2221–2233, 2020. doi: 10.1021/acsomega.9b03352. URL https://doi.org/10.1021/acsomega.9b03352. PMID: 32064383.

[29] Claire M. Belcher, Jonathan M. Yearsley, Rory M. Hadden, Jennifer C. McElwain, and Guillermo Rein. Baseline intrinsic flammability of earth's ecosystems estimated from paleoatmospheric oxygen over the past 350 million years. *Proceedings of the National Academy of Sciences*, 107(52):22448–22453, 2010. doi: 10.1073/pnas.1011974107. URL https://www.pnas.org/doi/abs/10.1073/pnas.1011974107.

[30] Jose V Moris, Matthew J Reilly, Zhiqiang Yang, Warren B Cohen, Renzo Motta, and Davide Ascoli. Using a trait-based approach to asses fire resistance in forest landscapes of the inland northwest, usa. *Landscape Ecology*, 37(8):2149–2164, 2022.

[31] Brendan M Rogers, Amber J Soja, Michael L Goulden, and James T Randerson. Influence of tree species on continental differences in boreal fires and climate feedbacks. *Nature Geoscience*, 8(3):228–234, 2015.

[32] WJ De Groot, PM Bothwell, DH Carlsson, and KA Logan. Simulating the effects of future fire regimes on western canadian boreal forests. *Journal of Vegetation Science*, 14(3):355–364, 2003.

[33] CE Van Wagner, Petawawa Forest, et al. Development and structure of the canadian forest fireweather index system. In *Can. For. Serv., Forestry Tech. Rep*. Citeseer, 1987.

[34] S. S. Rabin, J. R. Melton, G. Lasslop, D. Bachelet, M. Forrest, S. Hantson, J. O. Kaplan, F. Li, S. Mangeon, D. S. Ward, C. Yue, V. K. Arora, T. Hickler, S. Kloster, W. Knorr, L. Nieradzik, A. Spessa, G. A. Folberth, T. Sheehan, A. Voulgarakis, D. I. Kelley, I. C. Prentice, S. Sitch, S. Harrison, and A. Arneth. The fire modeling intercomparison project (firemip), phase 1: experimental and analytical protocols with detailed model descriptions. *Geoscientific Model Development*, 10(3):1175–1197, 2017. doi: 10.5194/gmd-10-1175-2017. URL https://gmd.copernicus.org/articles/10/1175/2017/.

[35] Eric S Kasischke, Edward J Hyer, Paul C Novelli, Lori P Bruhwiler, Nancy HF French, Anatoly I Sukhinin, Jennifer H Hewson, and Brian J Stocks. Influences of boreal fire emissions on northern hemisphere atmospheric carbon and carbon monoxide. *Global Biogeochemical Cycles*, 19(1), 2005.

[36] E. B. Wiggins, A. Andrews, C. Sweeney, J. B. Miller, C. E. Miller, S. Veraverbeke, R. Commane, S. Wofsy, J. M. Henderson, and J. T. Randerson. Evidence for a larger contribution of smoldering combustion to boreal forest fire emissions from tower observations in alaska. *Atmospheric Chemistry and Physics Discussions*, 2020:1–26, 2020. doi: 10.5194/acp-2019-1067. URL https://acp.copernicus.org/preprints/acp-2019-1067/.

[37] Shawn P. Urbanski, Wei Min Hao, and Stephen Baker. Chapter 4 chemical composition of wildland fire emissions. In Andrzej Bytnerowicz, Michael J. Arbaugh, Allen R. Riebau, and Christian Andersen, editors, *Wildland Fires and Air Pollution*, volume 8 of *Developments in Environmental Science*, pages 79–107. Elsevier, 2008. doi: https://doi.org/10.1016/S1474-8177(08)00004-1. URL https://www.sciencedirect.com/science/article/pii/S1474817708000041.

[38] Michael WI Schmidt and Angela G Noack. Black carbon in soils and sediments: analysis, distribution, implications, and current challenges. *Global biogeochemical cycles*, 14(3):777–793, 2000.

[39] Caroline M Preston and Michael WI Schmidt. Black (pyrogenic) carbon: a synthesis of current knowledge and uncertainties with special consideration of boreal regions. *Biogeosciences*, 3(4): 397–420, 2006.

[40] Lacey A. Pyle, William C. Hockaday, Thomas Boutton, Kyriacos Zygourakis, Timothy J. Kinney, and Caroline A. Masiello. Chemical and isotopic thresholds in charring: Implications for the interpretation of charcoal mass and isotopic data. *Environmental Science & Technology*, 49(24): 14057–14064, 2015. doi: 10.1021/acs.est.5b03087. URL https://doi.org/10.1021/acs.est.5b03087. PMID: 26523420.

[41] Steven D. Allison, Tracy B. Gartner, Michelle C. Mack, Krista McGuire, and Kathleen Treseder. Nitrogen alters carbon dynamics during early succession in boreal forest. *Soil Biology and Biochemistry*, 42(7):1157–1164, 2010. ISSN 0038-0717. doi: https://doi.org/10.1016/j.soilbio.2010.03.026. URL https://www.sciencedirect.com/science/article/pii/S0038071710001185.

[42] Alysha I Coppola, Sasha Wagner, Sinikka T Lennartz, Michael Seidel, Nicholas D Ward, Thorsten Dittmar, Cristina Santín, and Matthew W Jones. The black carbon cycle and its role in the earth system. *Nature Reviews Earth & Environment*, pages 1–17, 2022.

[43] Rodney J. Keenan, Gregory A. Reams, Frédéric Achard, Joberto V. de Freitas, Alan Grainger, and Erik Lindquist. Dynamics of global forest area: Results from the fao global forest resources assessment 2015. *Forest Ecology and Management*, 352:9–20, 2015. ISSN 0378-1127. doi: https://doi.org/10.1016/j.foreco.2015.06.014. URL https://www.sciencedirect.com/science/article/pii/S0378112715003400. Changes in Global Forest Resources from 1990 to 2015.

[44] Jörn PW Scharlemann, Edmund VJ Tanner, Roland Hiederer, and Valerie Kapos. Global soil carbon: understanding and managing the largest terrestrial carbon pool. *Carbon Management*, 5 (1):81–91, 2014. doi: 10.4155/cmt.13.77. URL https://doi.org/10.4155/cmt.13.77.

[45] Colin Averill, Benjamin L Turner, and Adrien C Finzi. Mycorrhiza-mediated competition between plants and decomposers drives soil carbon storage. *Nature*, 505(7484):543–545, 2014.

[46] Michael Bonkowski. Protozoa and plant growth: the microbial loop in soil revisited. *New Phytologist*, 162(3):617–631, 2004. doi: https://doi.org/10.1111/j.1469-8137.2004.01066.x. URL https://nph.onlinelibrary.wiley.com/doi/abs/10.1111/j.1469-8137.2004.01066.x.

[47] Oskar Franklin, Torgny Näsholm, Peter Högberg, and Mona N. Högberg. Forests trapped in nitrogen limitation – an ecological market perspective on ectomycorrhizal symbiosis. *New Phytologist*, 203(2):657–666, 2014. doi: https://doi.org/10.1111/nph.12840. URL https://nph.onlinelibrary.wiley.com/doi/abs/10.1111/nph.12840.

[48] Torgny Näsholm, Peter Högberg, Oskar Franklin, Daniel Metcalfe, Sonja G. Keel, Catherine Campbell, Vaughan Hurry, Sune Linder, and Mona N. Högberg. Are ectomycorrhizal fungi alleviating or aggravating nitrogen limitation of tree growth in boreal forests? *New Phytologist*, 198 (1):214–221, 2013. doi: https://doi.org/10.1111/nph.12139. URL https://nph.onlinelibrary.wiley.com/doi/abs/10.1111/nph.12139.

[49] K. E. Clemmensen, A. Bahr, O. Ovaskainen, A. Dahlberg, A. Ekblad, H. Wallander, J. Stenlid, R. D. Finlay, D. A. Wardle, and B. D. Lindahl. Roots and associated fungi drive long-term carbon sequestration in boreal forest. *Science*, 339(6127):1615–1618, 2013. doi: 10.1126/science.1231923. URL https://www.science.org/doi/abs/10.1126/science.1231923.

[50] Torbern Tagesson, Guy Schurgers, Stéphanie Horion, Philippe Ciais, Feng Tian, Martin Brandt, Anders Ahlström, Jean-Pierre Wigneron, Jonas Ardö, Stefan Olin, et al. Recent divergence in the contributions of tropical and boreal forests to the terrestrial carbon sink. *Nature Ecology & Evolution*, 4(2):202–209, 2020.

[51] XJ Walker, K Okano, LT Berner, R Massey, SJ Goetz, JF Johnstone, and MC Mack. Shifts in ecological legacies support hysteresis of stand type conversions in boreal forests. *Ecosystems*, pages 1–10, 2023.

[52] Zelalem A Mekonnen, William J Riley, James T Randerson, Robert F Grant, and Brendan M Rogers. Expansion of high-latitude deciduous forests driven by interactions between climate warming and fire. *Nature plants*, 5(9):952–958, 2019.

[53] Teresita M Porter, Emily Smenderovac, Dave Morris, and Lisa Venier. All boreal forest successional stages needed to maintain the full suite of soil biodiversity, community composition, and function following wildfire. *Scientific Reports*, 13(1):7978, 2023.

[54] Kohmei Kadowaki, Satoshi Yamamoto, Hirotoshi Sato, Akifumi Tanabe, Amane Hidaka, and Hirokazu Toju. Mycorrhizal fungi mediate the direction and strength of plant–soil feedbacks differently between arbuscular mycorrhizal and ectomycorrhizal communities. *Communications Biology*, 1, 11 2018. doi: 10.1038/s42003-018-0201-9.

[55] Malte Meinshausen, Nicolai Meinshausen, William Hare, Sarah CB Raper, Katja Frieler, Reto Knutti, David J Frame, and Myles R Allen. Greenhouse-gas emission targets for limiting global warming to 2 c. *Nature*, 458(7242):1158–1162, 2009.

[56] Intergovernmental Panel on Climate Change (IPCC). *Climate Change 2022: Impacts, Adaptation, and Vulnerability*. Cambridge University Press, Cambridge, UK and New York, NY, USA, 2021. doi: 10.1017/9781009325844.

[57] Mike Flannigan, Brian Stocks, Merritt Turetsky, and Mike Wotton. Impacts of climate change on fire activity and fire management in the circumboreal forest. *Global Change Biology*, 15(3):549–560, 2009. doi: https://doi.org/10.1111/j.1365-2486.2008.01660.x. URL `https://onlinelibrary.wiley.com/doi/abs/10.1111/j.1365-2486.2008.01660.x`.

[58] Jennifer L. Baltzer, Nicola J. Day, Xanthe J. Walker, David Greene, Michelle C. Mack, Heather D. Alexander, Dominique Arseneault, Jennifer Barnes, Yves Bergeron, Yan Boucher, Laura Bourgeau-Chavez, Carissa D. Brown, Suzanne Carrière, Brian K. Howard, Sylvie Gauthier, Marc-André Parisien, Kirsten A. Reid, Brendan M. Rogers, Carl Roland, Luc Sirois, Sarah Stehn, Dan K. Thompson, Merritt R. Turetsky, Sander Veraverbeke, Ellen Whitman, Jian Yang, and Jill F. Johnstone. Increasing fire and the decline of fire adapted black spruce in the boreal forest. *Proceedings of the National Academy of Sciences*, 118(45):e2024872118, 2021. doi: 10.1073/pnas.2024872118. URL `https://www.pnas.org/doi/abs/10.1073/pnas.2024872118`.

[59] William J de Groot, Alan S Cantin, Michael D Flannigan, Amber J Soja, Lynn M Gowman, and Alison Newbery. A comparison of canadian and russian boreal forest fire regimes. *Forest Ecology and Management*, 294:23–34, 2013.

[60] Cristina Santín, Stefan H. Doerr, Agustín Merino, Robert Bryant, and Neil J. Loader. Forest floor chemical transformations in a boreal forest fire and their correlations with temperature and heating duration. *Geoderma*, 264:71–80, 2016. ISSN 0016-7061. doi: https://doi.org/10.1016/j.geoderma.2015.09.021. URL `https://www.sciencedirect.com/science/article/pii/S001670611530094X`.

[61] A.A. Dymov, V.V. Startsev, E.Yu. Milanovsky, I.A. Valdes-Korovkin, Yu.R. Farkhodov, A.V. Yudina, O. Donnerhack, and G. Guggenberger. Soils and soil organic matter transforma-

tions during the two years after a low-intensity surface fire (subpolar ural, russia). *Geoderma*, 404:115278, 2021. ISSN 0016-7061. doi: https://doi.org/10.1016/j.geoderma.2021.115278. URL https://www.sciencedirect.com/science/article/pii/S001670612100358X.

[62] Arden L. Burrell, Qiaoqi Sun, Robert Baxter, Elena A. Kukavskaya, Sergey Zhila, Tatiana Shestakova, Brendan M. Rogers, Jörg Kaduk, and Kirsten Barrett. Climate change, fire return intervals and the growing risk of permanent forest loss in boreal eurasia. *Science of The Total Environment*, 831:154885, 2022. ISSN 0048-9697. doi: https://doi.org/10.1016/j.scitotenv.2022.154885. URL https://www.sciencedirect.com/science/article/pii/S0048969722019787.

[63] SC Zoltai, LA Morrissey, GP Livingston, and WJ de Groot. Effects of fires on carbon cycling in north american boreal peatlands. *Environmental Reviews*, 6(1):13–24, 1998.

[64] Amanda L Bataineh, Brian P Oswald, Mohammad Bataineh, Daniel Unger, I-Kuai Hung, and Daniel Scognamillo. Spatial autocorrelation and pseudoreplication in fire ecology. *Fire Ecology*, 2 (2):107–118, 2006. URL https://doi.org/10.4996/fireecology.0202107.

[65] David J. Currie. Where newton might have taken ecology. *Global Ecology and Biogeography*, 28(1): 18–27, 2019. doi: https://doi.org/10.1111/geb.12842. URL https://onlinelibrary.wiley.com/doi/abs/10.1111/geb.12842.

[66] F. Krikken, F. Lehner, K. Haustein, I. Drobyshev, and G. J. van Oldenborgh. Attribution of the role of climate change in the forest fires in sweden 2018. *Natural Hazards and Earth System Sciences*, 21(7):2169–2179, 2021. doi: 10.5194/nhess-21-2169-2021. URL https://nhess.copernicus.org/articles/21/2169/2021/.

[67] Naturvårdsverket. Markfuktighetsindex producerat som del av nationella marktäckedata, nmd 2018. https://metadatakatalogen.naturvardsverket.se/metadatakatalogen/GetMetaDataById?id=cae71f45-b463-447f-804f-2847869b19b0.

[68] B. P. Buchanan, M. Fleming, R. L. Schneider, B. K. Richards, J. Archibald, Z. Qiu, and M. T. Walter. Evaluating topographic wetness indices across central new york agricultural landscapes. *Hydrology and Earth System Sciences*, 18(8):3279–3299, 2014. doi: 10.5194/hess-18-3279-2014. URL https://hess.copernicus.org/articles/18/3279/2014/.

[69] Paul NC Murphy, Jae Ogilvie, Kevin Connor, and Paul A Arp. Mapping wetlands: a comparison of two different approaches for new brunswick, canada. *Wetlands*, 27(4):846–854, 2007. doi: 10.1672/0277-5212(2007)27[846:MWACOT]2.0.CO;2.

[70] K. J. Beven and M. J. Kirkby. A physically based, variable contributing area model of basin hydrology. *Hydrological Sciences Bulletin*, 24(1):43–69, 1979. doi: 10.1080/02626667909491834. URL https://doi.org/10.1080/02626667909491834.

[71] Lantmäteriet. Markhöjdmodell nedladdning, grid 50+. https://www.lantmateriet.se/sv/Kartor-och-geografisk-information/geodataprodukter/produktlista/markhojdmodell-nedladdning-grid-50/#steg=1, 2021.

[72] Esri Inc. *ArcGIS Pro*. Esri Inc., 2019. URL https://www.esri.com/en-us/arcgis/products/arcgis-pro/.

[73] Katja Sidoroff, Timo Kuuluvainen, Heidi Tanskanen, and Ilkka Vanha-Majamaa. Tree mortality after low-intensity prescribed fires in managed pinus sylvestris stands in southern finland. *Scandinavian Journal of Forest Research*, 22(1):2–12, 2007. doi: 10.1080/02827580500365935. URL https://doi.org/10.1080/02827580500365935.

[74] LG Marklund. Biomass functions for norway spruce (picea abies (l.) karst.) in sweden [biomass

determination, dry weight]. *Rapport-Sveriges Lantbruksuniversitet, Institutionen foer Skogstaxering (Sweden)*, 1987.

[75] Leslie A. Boby, Edward A. G. Schuur, Michelle C. Mack, David Verbyla, and Jill F. Johnstone. Quantifying fire severity, carbon, and nitrogen emissions in alaska's boreal forest. *Ecological Applications*, 20(6):1633–1647, 2010. doi: 10.1890/08-2295.1. URL https://esajournals.onlinelibrary.wiley.com/doi/abs/10.1890/08-2295.1.

[76] Samuel F. Bartels, Han Y.H. Chen, Michael A. Wulder, and Joanne C. White. Trends in post-disturbance recovery rates of canada's forests following wildfire and harvest. *Forest Ecology and Management*, 361:194–207, 2016. ISSN 0378-1127. doi: https://doi.org/10.1016/j.foreco.2015.11.015. URL https://www.sciencedirect.com/science/article/pii/S0378112715006386.

[77] Johnny Schimmel and Anders Granstrom. Fire severity and vegetation response in the boreal swedish forest. *Ecology*, 77(5):1436–1450, 1996. doi: https://doi.org/10.2307/2265541. URL https://esajournals.onlinelibrary.wiley.com/doi/abs/10.2307/2265541.

[78] O. A. Zyryanova, A. P. Abaimov, T. N. Bugaenko, and N. N. Bugaenko. *Recovery of Forest Vegetation After Fire Disturbance*, pages 83–96. Springer Netherlands, Dordrecht, 2010. ISBN 978-1-4020-9693-8. doi: 10.1007/978-1-4020-9693-8_5. URL https://doi.org/10.1007/978-1-4020-9693-8_5.

[79] A Granström and J Schimmel. Heat effects on seeds and rhizomes of a selection of boreal forest plants and potential reaction to fire. *Oecologia*, 94:307–313, 1993.

[80] Bengt Gunnar Jonsson, Magnus Ekström, Per-Anders Esseen, Anton Grafström, Göran Ståhl, and Bertil Westerlund. Dead wood availability in managed swedish forests – policy outcomes and implications for biodiversity. *Forest Ecology and Management*, 376:174–182, 2016. ISSN 0378-1127. doi: https://doi.org/10.1016/j.foreco.2016.06.017. URL https://www.sciencedirect.com/science/article/pii/S0378112716303140.

[81] Catherine M. Dieleman, Brendan M. Rogers, Stefano Potter, Sander Veraverbeke, Jill F. Johnstone, Jocelyne Laflamme, Kylen Solvik, Xanthe J. Walker, Michelle C. Mack, and Merritt R. Turetsky. Wildfire combustion and carbon stocks in the southern canadian boreal forest: Implications for a warming world. *Global Change Biology*, 26(11):6062–6079, 2020. doi: https://doi.org/10.1111/gcb.15158. URL https://onlinelibrary.wiley.com/doi/abs/10.1111/gcb.15158.

[82] Terje Kristensen, Mikael Ohlson, Paul Bolstad, and Zoltan Nagy. Spatial variability of organic layer thickness and carbon stocks in mature boreal forest stands—implications and suggestions for sampling designs. *Environmental monitoring and assessment*, 187(8):1–19, 2015. doi: 10.1007/s10661-015-4741-x. URL https://doi.org/10.1007/s10661-015-4741-x.

[83] Canadian Agricultural Services Coordinating Committee. *The Canadian system of soil classification*. NRC Research Press, 1998. ISBN 0-660-17404-9.

[84] Merche B. Bodí, Deborah A. Martin, Victoria N. Balfour, Cristina Santín, Stefan H. Doerr, Paulo Pereira, Artemi Cerdà, and Jorge Mataix-Solera. Wildland fire ash: Production, composition and eco-hydro-geomorphic effects. *Earth-Science Reviews*, 130:103–127, 2014. ISSN 0012-8252. doi: https://doi.org/10.1016/j.earscirev.2013.12.007. URL https://www.sciencedirect.com/science/article/pii/S0012825214000026.

[85] Stef Haesen, Jonas J. Lembrechts, Pieter De Frenne, Jonathan Lenoir, Juha Aalto, Michael B. Ashcroft, Martin Kopecký, Miska Luoto, Ilya Maclean, Ivan Nijs, Pekka Niittynen, Johan van den Hoogen, Nicola Arriga, Josef Brůna, Nina Buchmann, Marek Čiliak, Alessio Collalti, Emiel De Lombaerde, Patrice Descombes, Mana Gharun, Ignacio Goded, Sanne Govaert, Caroline

Greiser, Achim Grelle, Carsten Gruening, Lucia Hederová, Kristoffer Hylander, Jürgen Kreyling, Bart Kruijt, Martin Macek, František Máliš, Matěj Man, Giovanni Manca, Radim Matula, Camille Meeussen, Sonia Merinero, Stefano Minerbi, Leonardo Montagnani, Lena Muffler, Romà Ogaya, Josep Penuelas, Roman Plichta, Miguel Portillo-Estrada, Jonas Schmeddes, Ankit Shekhar, Fabien Spicher, Mariana Ujházyová, Pieter Vangansbeke, Robert Weigel, Jan Wild, Florian Zellweger, and Koenraad Van Meerbeek. Foresttemp – sub-canopy microclimate temperatures of european forests. *Global Change Biology*, 27(23):6307–6319, 2021. doi: https://doi.org/10.1111/gcb.15892. URL `https://onlinelibrary.wiley.com/doi/abs/10.1111/gcb.15892`.

[86] Jonas J. Lembrechts, Johan van den Hoogen, Juha Aalto, Michael B. Ashcroft, Pieter De Frenne, Julia Kemppinen, Martin Kopecký, Miska Luoto, Ilya M. D. Maclean, Thomas W. Crowther, Joseph J. Bailey, Stef Haesen, David H. Klinges, Pekka Niittynen, Brett R. Scheffers, Koenraad Van Meerbeek, Peter Aartsma, Otar Abdalaze, Mehdi Abedi, Rien Aerts, Negar Ahmadian, Antje Ahrends, Juha M. Alatalo, Jake M. Alexander, Camille Nina Allonsius, Jan Altman, Christof Ammann, Christian Andres, Christopher Andrews, Jonas Ardö, Nicola Arriga, Alberto Arzac, Valeria Aschero, Rafael L. Assis, Jakob Johann Assmann, Maaike Y. Bader, Khadijeh Bahalkeh, Peter Barančok, Isabel C. Barrio, Agustina Barros, Matti Barthel, Edmund W. Basham, Marijn Bauters, Manuele Bazzichetto, Luca Belelli Marchesini, Michael C. Bell, Juan C. Benavides, José Luis Benito Alonso, Bernd J. Berauer, Jarle W. Bjerke, Robert G. Björk, Mats P. Björkman, Katrin Björnsdóttir, Benjamin Blonder, Pascal Boeckx, Julia Boike, Stef Bokhorst, Bárbara N. S. Brum, Josef Brůna, Nina Buchmann, Pauline Buysse, José Luís Camargo, Otávio C. Campoe, Onur Candan, Rafaella Canessa, Nicoletta Cannone, Michele Carbognani, Jofre Carnicer, Angélica Casanova-Katny, Simone Cesarz, Bogdan Chojnicki, Philippe Choler, Steven L. Chown, Edgar F. Cifuentes, Marek Čiliak, Tamara Contador, Peter Convey, Elisabeth J. Cooper, Edoardo Cremonese, Salvatore R. Curasi, Robin Curtis, Maurizio Cutini, C. Johan Dahlberg, Gergana N. Daskalova, Miguel Angel de Pablo, Stefano Della Chiesa, Jürgen Dengler, Bart Deronde, Patrice Descombes, Valter Di Cecco, Michele Di Musciano, Jan Dick, Romina D. Dimarco, Jiri Dolezal, Ellen Dorrepaal, Jiří Dušek, Nico Eisenhauer, Lars Eklundh, Todd E. Erickson, Brigitta Erschbamer, Werner Eugster, Robert M. Ewers, Dan A. Exton, Nicolas Fanin, Fatih Fazlioglu, Iris Feigenwinter, Giuseppe Fenu, Olga Ferlian, M. Rosa Fernández Calzado, Eduardo Fernández-Pascual, Manfred Finckh, Rebecca Finger Higgens, T'ai G. W. Forte, Erika C. Freeman, Esther R. Frei, Eduardo Fuentes-Lillo, Rafael A. García, María B. García, Charly Géron, Mana Gharun, Dany Ghosn, Khatuna Gigauri, Anne Gobin, Ignacio Goded, Mathias Goeckede, Felix Gottschall, Keith Goulding, Sanne Govaert, Bente Jessen Graae, Sarah Greenwood, Caroline Greiser, Achim Grelle, Benoit Guénard, Mauro Guglielmin, Joannès Guillemot, Peter Haase, Sylvia Haider, Aud H. Halbritter, Maroof Hamid, Albin Hammerle, Arndt Hampe, Siri V. Haugum, Lucia Hederová, Bernard Heinesch, Carole Helfter, Daniel Hepenstrick, Maximiliane Herberich, Mathias Herbst, Luise Hermanutz, David S. Hik, Raúl Hoffrén, Jürgen Homeier, Lukas Hörtnagl, Toke T. Høye, Filip Hrbacek, Kristoffer Hylander, Hiroki Iwata, Marcin Antoni Jackowicz-Korczynski, Hervé Jactel, Järvi Järveoja, Szymon Jastrzębowski, Anke Jentsch, Juan J. Jiménez, Ingibjörg S. Jónsdóttir, Tommaso Jucker, Alistair S. Jump, Radoslaw Juszczak, Róbert Kanka, Vít Kašpar, George Kazakis, Julia Kelly, Anzar A. Khuroo, Leif Klemedtsson, Marcin Klisz, Natascha Kljun, Alexander Knohl, Johannes Kobler, Jozef Kollár, Martyna M. Kotowska, Bence Kovács, Juergen Kreyling, Andrea Lamprecht, Simone I. Lang, Christian Larson, Keith Larson, Kamil Laska, Guerric le Maire, Rachel I. Leihy, Luc Lens, Bengt Liljebladh, Annalea Lohila, Juan Lorite, Benjamin Loubet, Joshua Lynn, Martin Macek, Roy Mackenzie, Enzo Magliulo, Regine Maier, Francesco Malfasi, František Máliš, Matěj Man, Giovanni Manca, Antonio Manco, Tanguy Manise, Paraskevi Manolaki, Felipe Marciniak, Radim Matula, Ana Clara Mazzolari, Sergiy Medinets, Volodymyr Medinets, Camille Meeussen, Sonia Merinero, Rita de Cássia Guimarães Mesquita, Katrin Meusburger, Filip J. R. Meysman, Sean T. Michaletz, Ann Milbau, Dmitry Moiseev, Pavel Moiseev, Andrea Mondoni, Ruth Monfries, Leonardo Montagnani,

Mikel Moriana-Armendariz, Umberto Morra di Cella, Martin Mörsdorf, Jonathan R. Mosedale, Lena Muffler, Miriam Muñoz-Rojas, Jonathan A. Myers, Isla H. Myers-Smith, Laszlo Nagy, Marianna Nardino, Ilona Naujokaitis-Lewis, Emily Newling, Lena Nicklas, Georg Niedrist, Armin Niessner, Mats B. Nilsson, Signe Normand, Marcelo D. Nosetto, Yann Nouvellon, Martin A. Nuñez, Romà Ogaya, Jérôme Ogée, Joseph Okello, Janusz Olejnik, Jørgen Eivind Olesen, Øystein H. Opedal, Simone Orsenigo, Andrej Palaj, Timo Pampuch, Alexey V. Panov, Meelis Pärtel, Ada Pastor, Aníbal Pauchard, Harald Pauli, Marian Pavelka, William D. Pearse, Matthias Peichl, Loïc Pellissier, Rachel M. Penczykowski, Josep Penuelas, Matteo Petit Bon, Alessandro Petraglia, Shyam S. Phartyal, Gareth K. Phoenix, Casimiro Pio, Andrea Pitacco, Camille Pitteloud, Roman Plichta, Francesco Porro, Miguel Portillo-Estrada, Jérôme Poulenard, Rafael Poyatos, Anatoly S. Prokushkin, Radoslaw Puchalka, Mihai Pușcaș, Dajana Radujković, Krystal Randall, Amanda Ratier Backes, Sabine Remmele, Wolfram Remmers, David Renault, Anita C. Risch, Christian Rixen, Sharon A. Robinson, Bjorn J. M. Robroek, Adrian V. Rocha, Christian Rossi, Graziano Rossi, Olivier Roupsard, Alexey V. Rubtsov, Patrick Saccone, Clotilde Sagot, Jhonatan Sallo Bravo, Cinthya C. Santos, Judith M. Sarneel, Tobias Scharnweber, Jonas Schmeddes, Marius Schmidt, Thomas Scholten, Max Schuchardt, Naomi Schwartz, Tony Scott, Julia Seeber, Ana Cristina Segalin de Andrade, Tim Seipel, Philipp Semenchuk, Rebecca A. Senior, Josep M. Serra-Diaz, Piotr Sewerniak, Ankit Shekhar, Nikita V. Sidenko, Lukas Siebicke, Laura Siegwart Collier, Elizabeth Simpson, David P. Siqueira, Zuzana Sitková, Johan Six, Marko Smiljanic, Stuart W. Smith, Sarah Smith-Tripp, Ben Somers, Mia Vedel Sørensen, José João L. L. Souza, Bartolomeu Israel Souza, Arildo Souza Dias, Marko J. Spasojevic, James D. M. Speed, Fabien Spicher, Angela Stanisci, Klaus Steinbauer, Rainer Steinbrecher, Michael Steinwandter, Michael Stemkovski, Jörg G. Stephan, Christian Stiegler, Stefan Stoll, Martin Svátek, Miroslav Svoboda, Torbern Tagesson, Andrew J. Tanentzap, Franziska Tanneberger, Jean-Paul Theurillat, Haydn J. D. Thomas, Andrew D. Thomas, Katja Tielbörger, Marcello Tomaselli, Urs Albert Treier, Mario Trouillier, Pavel Dan Turtureanu, Rosamond Tutton, Vilna A. Tyystjärvi, Masahito Ueyama, Karol Ujházy, Mariana Ujházyová, Domas Uogintas, Anastasiya V. Urban, Josef Urban, Marek Urbaniak, Tudor-Mihai Ursu, Francesco Primo Vaccari, Stijn Van de Vondel, Liesbeth van den Brink, Maarten Van Geel, Vigdis Vandvik, Pieter Vangansbeke, Andrej Varlagin, G. F. Veen, Elmar Veenendaal, Susanna E. Venn, Hans Verbeeck, Erik Verbrugggen, Frank G. A. Verheijen, Luis Villar, Luca Vitale, Pascal Vittoz, Maria Vives-Ingla, Jonathan von Oppen, Josefine Walz, Runxi Wang, Yifeng Wang, Robert G. Way, Ronja E. M. Wedegärtner, Robert Weigel, Jan Wild, Matthew Wilkinson, Martin Wilmking, Lisa Wingate, Manuela Winkler, Sonja Wipf, Georg Wohlfahrt, Georgios Xenakis, Yan Yang, Zicheng Yu, Kailiang Yu, Florian Zellweger, Jian Zhang, Zhaochen Zhang, Peng Zhao, Klaudia Ziemblińska, Reiner Zimmermann, Shengwei Zong, Viacheslav I. Zyryanov, Ivan Nijs, and Jonathan Lenoir. Global maps of soil temperature. *Global Change Biology*, 28(9):3110–3144, 2022. doi: https://doi.org/10.1111/gcb.16060. URL `https://onlinelibrary.wiley.com/doi/abs/10.1111/gcb.16060`.

[87] Åsa Frostegård, Anders Tunlid, and Erland Bååth. Use and misuse of plfa measurements in soils. *Soil Biology and Biochemistry*, 43(8):1621–1625, 2011. ISSN 0038-0717. doi: https://doi.org/10.1016/j.soilbio.2010.11.021. URL `https://www.sciencedirect.com/science/article/pii/S0038071710004426`.

[88] Örjan Gustafsson and Philip M Gschwend. Soot as a strong partition medium for polycyclic aromatic hydrocarbons in aquatic systems. 1997.

[89] Örjan Gustafsson, Thomas D. Bucheli, Zofia Kukulska, Mette Andersson, Claude Largeau, Jean-Noël Rouzaud, Christopher M. Reddy, and Timothy I. Eglinton. Evaluation of a protocol for the quantification of black carbon in sediments. *Global Biogeochemical Cycles*, 15(4):881–890, 2001. doi: https://doi.org/10.1029/2000GB001380. URL `https://agupubs.onlinelibrary.wiley.com/doi/abs/10.1029/2000GB001380`.

[90] Marie Elmquist, Örjan Gustafsson, and Per Andersson. Quantification of sedimentary black carbon using the chemothermal oxidation method: an evaluation of ex situ pretreatments and standard additions approaches. *Limnology and Oceanography: Methods*, 2(12):417–427, 2004. doi: https://doi.org/10.4319/lom.2004.2.417. URL `https://aslopubs.onlinelibrary.wiley.com/doi/abs/10.4319/lom.2004.2.417`.

[91] Tripti Agarwal and Thomas D. Bucheli. Adaptation, validation and application of the chemothermal oxidation method to quantify black carbon in soils. *Environmental Pollution*, 159(2): 532–538, 2011. ISSN 0269-7491. doi: https://doi.org/10.1016/j.envpol.2010.10.012.

[92] Karen Hammes, Michael W. I. Schmidt, Ronald J. Smernik, Lloyd A. Currie, William P. Ball, Thanh H. Nguyen, Patrick Louchouarn, Stephane Houel, Örjan Gustafsson, Marie Elmquist, Gerard Cornelissen, Jan O. Skjemstad, Caroline A. Masiello, Jianzhong Song, Ping'an Peng, Siddhartha Mitra, Joshua C. Dunn, Patrick G. Hatcher, William C. Hockaday, Dwight M. Smith, Christoph Hartkopf-Fröder, Axel Böhmer, Burkhard Lüer, Barry J. Huebert, Wulf Amelung, Sonja Brodowski, Lin Huang, Wendy Zhang, Philip M. Gschwend, D. Xanat Flores-Cervantes, Claude Largeau, Jean-Noël Rouzaud, Cornelia Rumpel, Georg Guggenberger, Klaus Kaiser, Andrei Rodionov, Francisco J. Gonzalez-Vila, José A. Gonzalez-Perez, José M. de la Rosa, David A. C. Manning, Elisa López-Capél, and Luyi Ding. Comparison of quantification methods to measure fire-derived (black/elemental) carbon in soils and sediments using reference materials from soil, water, sediment and the atmosphere. *Global Biogeochemical Cycles*, 21(3), 2007. doi: https://doi.org/10.1029/2006GB002914. URL `https://agupubs.onlinelibrary.wiley.com/doi/abs/10.1029/2006GB002914`.

[93] Moritz Reisser, Ross S Purves, Michael WI Schmidt, and Samuel Abiven. Pyrogenic carbon in soils: a literature-based inventory and a global estimation of its content in soil organic carbon and stocks. *Frontiers in Earth Science*, 4:80, 2016.

[94] E. G. Bligh and W. J. Dyer. A rapid method of total lipid extraction and purification. *Canadian Journal of Biochemistry and Physiology*, 37(8):911–917, 1959. doi: 10.1139/o59-099. URL `https://doi.org/10.1139/o59-099`. PMID: 13671378.

[95] DC White, WM Davis, JS Nickels, JD King, and RJ Bobbie. Determination of the sedimentary microbial biomass by extractable lipid phosphate. *Oecologia*, 40(1):51–62, 1979. doi: 10.1007/BF00388810.

[96] Rainer Georg Joergensen. Phospholipid fatty acids in soil—drawbacks and future prospects. *Biology and Fertility of Soils*, 58(1):1–6, 2022.

[97] Yingying Zhang, Ningguo Zheng, Juan Wang, Huaiying Yao, Qiongfen Qiu, and Stephen J. Chapman. High turnover rate of free phospholipids in soil confirms the classic hypothesis of plfa methodology. *Soil Biology and Biochemistry*, 135:323–330, 2019. ISSN 0038-0717. doi: https://doi.org/10.1016/j.soilbio.2019.05.023. URL `https://www.sciencedirect.com/science/article/pii/S0038071719301579`.

[98] C. Willers, P.J. Jansen van Rensburg, and S. Claassens. Phospholipid fatty acid profiling of microbial communities–a review of interpretations and recent applications. *Journal of Applied Microbiology*, 119(5):1207–1218, 2015. doi: https://doi.org/10.1111/jam.12902. URL `https://sfamjournals.onlinelibrary.wiley.com/doi/abs/10.1111/jam.12902`.

[99] Nicolas Fanin, Paul Kardol, Mark Farrell, Marie-Charlotte Nilsson, Michael J. Gundale, and David A. Wardle. The ratio of gram-positive to gram-negative bacterial plfa markers as an indicator of carbon availability in organic soils. *Soil Biology and Biochemistry*, 128:111–114, 2019. ISSN 0038-0717. doi: https://doi.org/10.1016/j.soilbio.2018.10.010. URL `https://www.sciencedirect.com/science/article/pii/S0038071718303584`.

[100] L Zelles. Fatty acid patterns of phospholipids and lipopolysaccharides in the characterisation of microbial communities in soil: a review. *Biology and fertility of soils*, 29(2):111–129, 1999.

[101] Deliang Chen, Peng Zhang, Kristina Seftigen, Tinghai Ou, Markus Giese, and Roland Barthel. Hydroclimate changes over sweden in the twentieth and twenty-first centuries: a millennium perspective. *Geografiska Annaler: Series A, Physical Geography*, 103(2):103–131, 2021. doi: 10.1080/04353676.2020.1841410. URL `https://doi.org/10.1080/04353676.2020.1841410`.

[102] Evgenii I. Ponomarev, Viacheslav I. Kharuk, and Kenneth J. Ranson. Wildfires dynamics in siberian larch forests. *Forests*, 7(6), 2016. ISSN 1999-4907. doi: 10.3390/f7060125. URL `https://www.mdpi.com/1999-4907/7/6/125`.

[103] Santiago Beguería, Borja Latorre, Fergus Reig, and Sergio M. Vicente-Serrarno. Global spei database, 2019. URL `https://spei.csic.es/database.html`.

[104] Pauli Virtanen, Ralf Gommers, Travis E. Oliphant, Matt Haberland, Tyler Reddy, David Cournapeau, Evgeni Burovski, Pearu Peterson, Warren Weckesser, Jonathan Bright, Stéfan J. van der Walt, Matthew Brett, Joshua Wilson, K. Jarrod Millman, Nikolay Mayorov, Andrew R. J. Nelson, Eric Jones, Robert Kern, Eric Larson, C J Carey, İlhan Polat, Yu Feng, Eric W. Moore, Jake VanderPlas, Denis Laxalde, Josef Perktold, Robert Cimrman, Ian Henriksen, E. A. Quintero, Charles R. Harris, Anne M. Archibald, Antônio H. Ribeiro, Fabian Pedregosa, Paul van Mulbregt, and SciPy 1.0 Contributors. SciPy 1.0: Fundamental Algorithms for Scientific Computing in Python. *Nature Methods*, 17:261–272, 2020. URL `https://doi.org/10.1038/s41592-019-0686-2`.

[105] Skipper Seabold and Josef Perktold. statsmodels: Econometric and statistical modeling with python. In *9th Python in Science Conference*, 2010.

[106] Kenneth P Burnham and David R Anderson. Multimodel inference: understanding aic and bic in model selection. *Sociological methods & research*, 33(2):261–304, 2004.

[107] Jari Oksanen, Gavin L. Simpson, F. Guillaume Blanchet, Roeland Kindt, Pierre Legendre, Peter R. Minchin, R.B. O'Hara, Peter Solymos, M. Henry H. Stevens, Eduard Szoecs, Helene Wagner, Matt Barbour, Michael Bedward, Ben Bolker, Daniel Borcard, Gustavo Carvalho, Michael Chirico, Miquel De Caceres, Sebastien Durand, Heloisa Beatriz Antoniazi Evangelista, Rich FitzJohn, Michael Friendly, Brendan Furneaux, Geoffrey Hannigan, Mark O. Hill, Leo Lahti, Dan McGlinn, Marie-Helene Ouellette, Eduardo Ribeiro Cunha, Tyler Smith, Adrian Stier, Cajo J.F. Ter Braak, and James Weedon. *vegan: Community Ecology Package*, 2022. URL `https://CRAN.R-project.org/package=vegan`. R package version 2.6-4.

[108] Xanthe J Walker, Jennifer L Baltzer, Steven G Cumming, Nicola J Day, Christopher Ebert, Scott Goetz, Jill F Johnstone, Stefano Potter, Brendan M Rogers, Edward AG Schuur, et al. Increasing wildfires threaten historic carbon sink of boreal forest soils. *Nature*, 572(7770):520–523, 2019.

[109] D. van Wees, G. R. van der Werf, J. T. Randerson, B. M. Rogers, Y. Chen, S. Veraverbeke, L. Giglio, and D. C. Morton. Global biomass burning fuel consumption and emissions at 500 m spatial resolution based on the global fire emissions database (gfed). *Geoscientific Model Development*, 15(22):8411–8437, 2022. doi: 10.5194/gmd-15-8411-2022. URL `https://gmd.copernicus.org/articles/15/8411/2022/`.

[110] Daniel A. Jaffe, Susan M. O'Neill, Narasimhan K. Larkin, Amara L. Holder, David L. Peterson, Jessica E. Halofsky, and Ana G. Rappold. Wildfire and prescribed burning impacts on air quality in the united states. *Journal of the Air & Waste Management Association*, 70(6):583–615, 2020. doi: 10.1080/10962247.2020.1749731. URL `https://doi.org/10.1080/10962247.2020.1749731`. PMID: 32240055.

[111] Carolyn Black, Yohannes Tesfaigzi, Jed A. Bassein, and Lisa A. Miller. Wildfire smoke expo-

sure and human health: Significant gaps in research for a growing public health issue. *Environmental Toxicology and Pharmacology*, 55:186–195, 2017. ISSN 1382-6689. doi: https://doi.org/10.1016/j.etap.2017.08.022. URL https://www.sciencedirect.com/science/article/pii/S1382668917302478.

[112] Hugh G. Smith, Gary J. Sheridan, Patrick N.J. Lane, Petter Nyman, and Shane Haydon. Wildfire effects on water quality in forest catchments: A review with implications for water supply. *Journal of Hydrology*, 396(1):170–192, 2011. ISSN 0022-1694. doi: https://doi.org/10.1016/j.jhydrol.2010.10.043. URL https://www.sciencedirect.com/science/article/pii/S0022169410006748.

[113] Federico Filipponi. Bais2: Burned area index for sentinel-2. In *Proceedings*, volume 2, page 364. MDPI, 2018.

[114] Nancy HF French, Pierre Goovaerts, and Eric S Kasischke. Uncertainty in estimating carbon emissions from boreal forest fires. *Journal of Geophysical Research: Atmospheres*, 109(D14), 2004.

[115] Amber J Soja, W Randy Cofer, Herman H Shugart, Anatoly I Sukhinin, Paul W Stackhouse, Douglas J McRae, and Susan G Conard. Estimating fire emissions and disparities in boreal siberia (1998–2002). *Journal of Geophysical Research: Atmospheres*, 109(D14), 2004.

[116] G. R. van der Werf, J. T. Randerson, L. Giglio, T. T. van Leeuwen, Y. Chen, B. M. Rogers, M. Mu, M. J. E. van Marle, D. C. Morton, G. J. Collatz, R. J. Yokelson, and P. S. Kasibhatla. Global fire emissions estimates during 1997–2016. *Earth System Science Data*, 9(2):697–720, 2017. doi: 10.5194/essd-9-697-2017. URL https://essd.copernicus.org/articles/9/697/2017/.

[117] S. Veraverbeke, B. M. Rogers, and J. T. Randerson. Daily burned area and carbon emissions from boreal fires in alaska. *Biogeosciences*, 12(11):3579–3601, 2015. doi: 10.5194/bg-12-3579-2015. URL https://bg.copernicus.org/articles/12/3579/2015/.

[118] J. W. Kaiser, A. Heil, M. O. Andreae, A. Benedetti, N. Chubarova, L. Jones, J.-J. Morcrette, M. Razinger, M. G. Schultz, M. Suttie, and G. R. van der Werf. Biomass burning emissions estimated with a global fire assimilation system based on observed fire radiative power. *Biogeosciences*, 9(1):527–554, 2012. doi: 10.5194/bg-9-527-2012. URL https://bg.copernicus.org/articles/9/527/2012/.

[119] XJ Walker, BM Rogers, S Veraverbeke, JF Johnstone, JL Baltzer, K Barrett, Laura Bourgeau-Chavez, NJ Day, WJ de Groot, CM Dieleman, et al. Fuel availability not fire weather controls boreal wildfire severity and carbon emissions. *Nature Climate Change*, pages 1–7, 2020.

[120] Claudia I. Czimczik and Caroline A. Masiello. Controls on black carbon storage in soils. *Global Biogeochemical Cycles*, 21(3), 2007. doi: https://doi.org/10.1029/2006GB002798. URL https://agupubs.onlinelibrary.wiley.com/doi/abs/10.1029/2006GB002798.

[121] S.-L. Bellè, A. A. Berhe, F. Hagedorn, C. Santin, M. Schiedung, I. van Meerveld, and S. Abiven. Key drivers of pyrogenic carbon redistribution during a simulated rainfall event. *Biogeosciences*, 18(3):1105–1126, 2021. doi: 10.5194/bg-18-1105-2021. URL https://bg.copernicus.org/articles/18/1105/2021/.

[122] G. Granath, C. D. Evans, J. Strengbom, J. Fölster, A. Grelle, J. Strömqvist, and S. J. Köhler. The impact of wildfire on biogeochemical fluxes and water quality in boreal catchments. *Biogeosciences*, 18(10):3243–3261, 2021. doi: 10.5194/bg-18-3243-2021. URL https://bg.copernicus.org/articles/18/3243/2021/.

[123] Rudolf Jaffé, Yan Ding, Jutta Niggemann, Anssi V. Vähätalo, Aron Stubbins, Robert G. M. Spencer, John Campbell, and Thorsten Dittmar. Global charcoal mobilization from soils

via dissolution and riverine transport to the oceans. *Science*, 340(6130):345–347, 2013. doi: 10.1126/science.1231476.

[124] Matthew W Jones, Alysha I Coppola, Cristina Santín, Thorsten Dittmar, Rudolf Jaffé, Stefan H Doerr, and Timothy A Quine. Fires prime terrestrial organic carbon for riverine export to the global oceans. *Nature communications*, 11(1):1–8, 2020.

[125] Anna V. McBeath, Ronald J. Smernik, Maximilian P.W. Schneider, Michael W.I. Schmidt, and Emma L. Plant. Determination of the aromaticity and the degree of aromatic condensation of a thermosequence of wood charcoal using nmr. *Organic Geochemistry*, 42(10):1194–1202, 2011. ISSN 0146-6380. doi: https://doi.org/10.1016/j.orggeochem.2011.08.008. URL `https://www.sciencedirect.com/science/article/pii/S0146638011002294`.

[126] Daniel B. Wiedemeier, Samuel Abiven, William C. Hockaday, Marco Keiluweit, Markus Kleber, Caroline A. Masiello, Anna V. McBeath, Peter S. Nico, Lacey A. Pyle, Maximilian P.W. Schneider, Ronald J. Smernik, Guido L.B. Wiesenberg, and Michael W.I. Schmidt. Aromaticity and degree of aromatic condensation of char. *Organic Geochemistry*, 78:135–143, 2015. ISSN 0146-6380. doi: https://doi.org/10.1016/j.orggeochem.2014.10.002. URL `https://www.sciencedirect.com/science/article/pii/S0146638014002587`.

[127] Matthew Jones, Cristina Santín, Guido Werf, and S.H. Doerr. Global fire emissions buffered by the production of pyrogenic carbon. *Nature Geoscience*, 12, 09 2019. doi: 10.1038/s41561-019-0403-x.

[128] Tripti Agarwal and Thomas D. Bucheli. Adaptation, validation and application of the chemothermal oxidation method to quantify black carbon in soils. *Environmental Pollution*, 159(2): 532–538, 2011. ISSN 0269-7491. doi: https://doi.org/10.1016/j.envpol.2010.10.012.

[129] Cristina Santín, Stefan H. Doerr, Caroline M. Preston, and Gil González-Rodríguez. Pyrogenic organic matter production from wildfires: a missing sink in the global carbon cycle. *Global Change Biology*, 21(4):1621–1633, 2015. doi: https://doi.org/10.1111/gcb.12800. URL `https://onlinelibrary.wiley.com/doi/abs/10.1111/gcb.12800`.

[130] Noémie A. Pichon, Elina Kaarlejärvi, and Anu Eskelinen. Seed limitation interacts with biotic and abiotic factors to constrain novel species' impact on community biomass and richness. *Ecology Letters*, 26(6):908–918, 2023. doi: https://doi.org/10.1111/ele.14219. URL `https://onlinelibrary.wiley.com/doi/abs/10.1111/ele.14219`.

[131] Carissa D. Brown, Juxin Liu, Guohua Yan, and Jill F. Johnstone. Disentangling legacy effects from environmental filters of postfire assembly of boreal tree assemblages. *Ecology*, 96(11):3023–3032, 2015. doi: https://doi.org/10.1890/14-2302.1. URL `https://esajournals.onlinelibrary.wiley.com/doi/abs/10.1890/14-2302.1`.

[132] Nicola J Day, Jill F Johnstone, Kirsten A Reid, Steven G Cumming, Michelle C Mack, Merritt R Turetsky, Xanthe J Walker, and Jennifer L Baltzer. Material legacies and environmental constraints underlie fire resilience of a dominant boreal forest type. *Ecosystems*, 26(3):473–490, 2023.

[133] Marie-Charlotte Nilsson and David A. Wardle. Understory vegetation as a forest ecosystem driver: evidence from the northern swedish boreal forest. *Frontiers in Ecology and the Environment*, 3(8): 421–428, 2005. doi: https://doi.org/10.1890/1540-9295(2005)003[0421:UVAAFE]2.0.CO;2.

Avhandlingar från Institutionen för naturgeografi och ekosystemanalys (INES), Lunds universitet

----

Dissertations from Department of Physical Geography and Ecosystem Science, University of Lund

---

Martin Sjöström, 2012: Satellite remote sensing of primary production in semi-arid Africa.

Zhenlin Yang, 2012: Small-scale climate variability and its ecosystem impacts in the sub-Arctic.

Ara Toomanian, 2012: Methods to improve and evaluate spatial data infrastructures.

Michal Heliasz, 2012: Spatial and temporal dynamics of subarctic birch forest carbon exchange.

Abdulghani Hasan, 2012: Spatially distributed hydrological modelling: wetness derived from digital elevation models to estimate peatland carbon.

Julia Bosiö, 2013: A green future with thawing permafrost mires?: a study of climate-vegetation interactions in European subarctic peatlands. (Lic.)

Anders Ahlström, 2013: Terrestrial ecosystem interactions with global climate and socio-economics.

Kerstin Baumanns, 2013: Drivers of global land use change: are increasing demands for food and bioenergy offset by technological change and yield increase? (Lic.)

Yengoh Genesis Tambang, 2013: Explaining agricultural yield gaps in Cameroon.

Jörgen Olofsson, 2013: The Earth: climate and anthropogenic interactions in a long time perspective.

David Wårlind, 2013: The role of carbon-nitrogen interactions for terrestrial ecosystem dynamics under global change: a modelling perspective.

Elin Sundqvist, 2014: Methane exchange in a boreal forest: the role of soils, vegetation and forest management.

Julie Mari Falk, 2014: Plant-soil-herbivore interactions in a high Arctic wetland: feedbacks to the carbon cycle.

Finn Hedefalk, 2014: Life histories across space and time: methods for including geographic factors on the micro-level in longitudinal demographic research. (Lic.)

Sadegh Jamali, 2014: Analyzing vegetation trends with sensor data from earth observation satellites.

Cecilia Olsson, 2014: Tree phenology modelling in the boreal and temperate climate zones : timing of spring and autumn events.

Jing Tang, 2014: Linking distributed hydrological processes with ecosystem vegetation dynamics and carbon cycling: modelling studies in a subarctic catchment of northern Sweden.

Wenxin Zhang, 2015: The role of biogeophysical feedbacks and their impacts in the arctic and boreal climate system.

Lina Eklund, 2015: "No Friends but the Mountains": understanding population mobility and land dynamics in Iraqi Kurdistan.

Stefan Olin, 2015: Ecosystems in the Anthropocene: the role of cropland management for carbon and nitrogen cycle processes.

Thomas Möckel, 2015: Hyperspectral and multispectral remote sensing for mapping grassland vegetation.

Hongxiao Jin, 2015: Remote sensing phenology at European northern latitudes: from ground spectral towers to satellites.

Bakhtiyor Pulatov, 2015: Potential impact of climate change on European agriculture: a case study of potato and Colorado potato beetle.

Christian Stiegler, 2016: Surface energy exchange and land-atmosphere interactions of Arctic and subarctic tundra ecosystems under climate change.

Per-Ola Olsson, 2016: Monitoring insect defoliation in forests with time-series of satellite based remote sensing data: near real-time methods and impact on the carbon balance.

Jonas Dalmayne, 2016: Monitoring biodiversity in cultural landscapes: development of remote sensing- and GIS-based methods.

Balathandayuthabani Panneer Selvam, 2016: Reactive dissolved organic carbon dynamics in a changing environment: experimental evidence from soil and water.

Kerstin Engström, 2016: Pathways to future cropland: assessing uncertainties in socio-economic processes by applying a global land-use model.

Finn Hedefalk, 2016: Life paths through space and time: adding the micro-level geographic context to longitudinal historical demographic research.

Ehsan Abdolmajidi, 2016: Modeling and improving Spatial Data Infrastructure (SDI).

Giuliana Zanchi, 2016: Modelling nutrient transport from forest ecosystems to surface waters.

Florian Sallaba, 2016: Biophysical and human controls of land productivity under global change: development and demonstration of parsimonious modelling techniques.

Norbert Pirk, 2017: Tundra meets atmosphere: seasonal dynamics of trace gas exchange in the High Arctic.

Minchao Wu, 2017: Land-atmosphere interactions and regional Earth system dynamics due to natural and anthropogenic vegetation changes.

Niklas Boke-Olén, 2017: Global savannah phenology: integrating earth observation, ecosystem modelling, and PhenoCams.

Abdulhakim M. Abdi, 2017: Primary production in African drylands: quantifying supply and demand using earth observation and socio-ecological data.

Nitin Chaudhary, 2017: Peatland dynamics in response to past and potential future climate change.

Ylva van Meeningen, 2017: Is genetic diversity more important for terpene emissions than latitudinal adaptation?: using genetically identical trees to better understand emission fluctuations across a European latitudinal gradient.

Patrik Vestin, 2017: Effects of forest management on greenhouse gas fluxes in a boreal forest.

Mohammadreza Rajabi, 2017: Spatial modeling and simulation for disease surveillance.

Jan Blanke, 2018: European ecosystems on a changing planet: integrating climate change and land-use intensity data.

Min Wang, 2018: Characteristics of BVOC emissions from a Swedish boreal forest: using chambers to capture biogenic volatile organic compounds (BVOCs) from trees and forest floor.

Wilhelm Dubber, 2018: Natural and social dimensions of forest carbon accounting.

Emma Johansson, 2018: Large-Scale Land Acquisitions as a Driver of Socio-Environmental Change: From the Pixel to the Globe.

Helen Eriksson, 2018: Harmonisation of geographic data: between geographic levels, hierarcic structures and over time. (Lic.)

Zhendong Wu, 2018: Modelling the terrestrial carbon cycle: drivers, benchmarks, and model-data fusion.

Zhanzhang Cai, 2019: Vegetation observation in the big data era: Sentinel-2 data for mapping the seasonality of land vegetation.

Fabien Rizinjirabake, 2019: Dissolved organic carbon in tropical watersheds: linking field observation and ecohydrological modelling.

Jeppe Ågård Kristensen, 2019: Biogeochemistry in Subarctic birch forests: perspectives on insect herbivory.

Yanzi Yan, 2019: The role of hydrological cycle in forest ecosystems: flow path, nutrient cycling and water-carbon interaction.

George Oriangi, 2019: Urban resilience to climate change shocks and stresses in Mbale municipality in Eastern Uganda.

Alex Paulo Lubida, 2019: Investigating spatial data infrastructure planning in Tanzania using system modelling and social concepts.

Weiming Huang, 2020: Geospatial data and knowledge on the Web: knowledge-based geospatial data integration and visualisation with Semantic Web technologies.

Oskar Löfgren, 2020: Remote sensing of grassland communities: integrated effects of soil nutrients and habitat age.

Altaaf Mechiche-Alami, 2020: Food security in a changing climate: the role of cropland intensification and land acquisitions across Africa.

Helen Eriksson, 2020: Harmonisation of 3D geodata – a prerequisite for a digital information flow for applications in the planning and building sector.

Augustus Aturinde, 2020: GIS and Health: Enhancing Disease Surveillance and Intervention through Spatial Epidemiology.

Geert Hensgens, 2020: Dissolved organic matter dynamics across terrestrial and aquatic systems: sources, chemistry and microbial processing.

Enass Said Al-Kharusi, 2021: Broad-Scale Patterns in CDOM and Total Organic Matter Concentrations of Inland Waters – Insights from Remote Sensing and GIS.

Tetiana Svystun, 2021: Understanding the environmental regulation of tree phenology.

Pearl Mzobe, 2021: Bearing the brunt of warming: Interactions between carbon and hydrology in northern Sweden.

Tomas Karlsson, 2021: The variability in Salix BVOC emissions and possible consequences for managed SRC plantations.

Olive Niyomubyeyi, 2022: Metaheuristic Algorithms for Spatial Multi-Objective Decision Making.

Veronika Kronnäs, 2022: Modelling effects of climate change and forestry on weathering rates and base cation cycling in forest soils.

Didac Pascual, 2022: The Torneträsk System - A basis for predicting future subarctic ecosystems.

Bernice Hwang, 2022: Impacts and drivers of insect herbivory on element cycling in forests globally.

Joel White, 2023: The functional potential of methane producing and consuming microorganisms in a changing world.

Alexandra Pongracz, 2023: Quantifying the impact of winter warming on the Arctic carbon cycle.

Sofia Junttila, 2023: Modelling carbon uptake in Nordic forest landscapes using remote sensing.

Deepak Waman, 2023: Mechanisms for the Influence from Ice Nucleus Aerosols on Clouds and their indirect effects: Cloud modelling.

Deborah Zani, 2023: Extending dynamic vegetation models to simulate range shifts.

Akash Deshmukh, 2023: Secondary ice production: An empirical formulation and organization of mechanisms among simulated cloud-types.

Johan Eckdahl, 2024: Boreal Forest Wildfire in a Changing Climate.

Department of Physical Geography
and Ecosystem Science
Faculty of Science

ISBN 978-91-89187-31-3